© 2020. Published by The Company of Biologists Ltd | Development (2020) 147, dev189647. doi:10.1242/dev.189647

RESEARCH ARTICLE

WRKY55 transcription factor positively regulates leaf senescence and the defense response by modulating the transcription of genes implicated in the biosynthesis of reactive oxygen species and salicylic acid in *Arabidopsis*

Yiqiao Wang*, Xing Cui*, Bo Yang*, Shutao Xu, Xiangyan Wei, Peiyu Zhao, Fangfang Niu, Mengting Sun, Chen Wang, Hao Cheng and Yuan-Qing Jiang‡

ABSTRACT

Reactive oxygen species (ROS) and salicylic acid (SA) are two factors regulating leaf senescence and defense against pathogens. However, how a single gene integrates both ROS and SA pathways remains poorly understood. Here, we show that *Arabidopsis* WRKY55 transcription factor positively regulates ROS and SA accumulation, and thus leaf senescence and resistance against the bacterial pathogen *Pseudomonas syringae*. *WRKY55* is predominantly expressed in senescent leaves and encodes a transcriptional activator localized to nuclei. Both inducible and constitutive overexpression of *WRKY55* accelerates leaf senescence, whereas mutants delay it. Transcriptomic sequencing identified 1448 differentially expressed genes, of which 1157 genes are upregulated by *WRKY55* expression. Accordingly, the ROS and SA contents in *WRKY55*-overexpressing plants are higher than those in control plants, whereas the opposite occurs in mutants. Moreover, WRKY55 positively regulates defense against *P. syringae*. Finally, we show that WRKY55 activates the expression of *RbohD*, *ICS1*, *PBS3* and *SAG13* by binding directly to the W-box-containing fragments. Taken together, our work has identified a new WRKY transcription factor that integrates both ROS and SA pathways to regulate leaf senescence and pathogen resistance.

KEY WORDS: *Arabidopsis*, WRKY55, Reactive oxygen species, Salicylic acid, Leaf senescence, Bacterial pathogen

INTRODUCTION

Leaf senescence occurs at the final stage of leaf development and precedes cell death, and it occurs not only with aging, but also in stressed or detached leaves (Woo et al., 2019). Past studies have demonstrated that leaf senescence is a highly coordinated process that mediates metabolite redistribution and reproductive maturation, eventually leading to cellular and organismal disintegration (Lim et al., 2007). Environmental stresses, such as salinity and drought, also induce premature leaf senescence by changing gene expression and physiological activities (Zhang and Zhou, 2013). Besides, some specific phytohormones, such as abscisic acid, ethylene (ET), jasmonic acid (JA) and salicylic acid (SA), have been shown to promote leaf senescence, whereas cytokinins and auxin can delay leaf senescence (Guo and Gan, 2005; Lim et al., 2007; Woo et al., 2019). Leaf senescence is regulated by transcriptional reprogramming of a large number of senescence-associated genes (SAGs), which are upregulated during senescence in *Arabidopsis* (*Arabidopsis thaliana*) (Breeze et al., 2011; Gepstein et al., 2003). SAG-encoded proteins play roles in macromolecule degradation, nutrient recycling and transport, detoxification of oxidative metabolites, induction of defense and establishment of stress tolerance (Gepstein et al., 2003). In senescent leaves of *Arabidopsis*, >100 transcription factor (TF) genes from various families, including NAC and WRKY, are upregulated (Balazadeh et al., 2008; Breeze et al., 2011; Guo et al., 2004), suggesting that transcriptional regulation is an essential step in this process.

The WRKY TF family comprises 72 members in *Arabidopsis* (Rushton et al., 2010). WRKY TFs could act as either transcriptional activators or repressors and regulate target gene expression through binding to the conserved W-box element (T)TGACC/T in the promoter regions (Ülker and Somssich, 2004). WRKY genes are the second largest group of TF genes in the *Arabidopsis* senescence transcriptome (Breeze et al., 2011; Guo et al., 2004), and a previous northern blotting analysis also revealed that 49 of the 72 *AtWRKY* genes were differentially expressed when infected by an avirulent strain of the bacterial pathogen *Pseudomonas syringae* pv. *tomato* with the *avrRpt2* gene or treated with a high concentration (2 mM) of SA (Dong et al., 2003). So far, functional analyses have shown that a few WRKY TFs from *Arabidopsis* positively or negatively regulate leaf senescence (Besseau et al., 2012; Guo et al., 2017; Jiang et al., 2014; Li et al., 2012; Miao et al., 2004; Robatzek and Somssich, 2001; Zhang et al., 2017) and provide defense against *P. syringae* (Kim et al., 2006; Sarris et al., 2015; Xu et al., 2006). For instance, AtWRKY57 functions as a node of convergence for JA- and auxin-mediated signaling in JA-induced leaf senescence (Jiang et al., 2014). WRKY45 acts through a gibberellin (GA)-mediated signaling pathway as a positive regulator of age-triggered leaf senescence (Chen et al., 2017). WRKY25 acts as a positive regulator of *WRKY53* expression, and WRKY25 itself negatively regulates leaf senescence (Doll et al., 2020). However, whether and how a single WRKY TF regulates both leaf senescence and defense response remain largely elusive.

State Key Laboratory of Soil Erosion and Dryland Farming on the Loess Plateau, College of Life Sciences, Northwest A&F University, Yangling, Shaanxi 712100, China.
*These authors contributed equally to this work

‡Author for correspondence (jiangyq@nwafu.edu.cn)

Y.W., 0000-0001-8179-5797; X.C., 0000-0003-1981-412X; B.Y., 0000-0002-0421-3754; S.X., 0000-0001-8525-2618; X.W., 0000-0002-8206-3691; P.Z., 0000-0002-4034-3994; F.N., 0000-0002-2249-764X; M.S., 0000-0002-8517-8451; C.W., 0000-0002-9841-2067; H.C., 0000-0002-1088-9777; Y.-Q.J., 0000-0003-1367-922X

Handling Editor: Ykä Helariutta
Received 19 February 2020; Accepted 13 July 2020

Development (2020) 147, dev189647. doi:10.1242/dev.189647

Reactive oxygen species (ROS) have multifaceted functions in growth, development, abiotic stress responses and immune response (Baxter et al., 2014; Suzuki et al., 2012). Homologs of mammalian NADPH oxidases, namely respiratory burst oxidase homologs (Rbohs), localized at the plasma membrane, play a crucial role in apoplastic ROS production (Torres and Dangl, 2005). The *Arabidopsis* genome contains 10 Rboh genes, namely *AtRbohA*-*AtRbohJ* (Torres and Dangl, 2005). Specifically, AtRbohD is the major constitutively active form, whereas expression of *AtRbohF* is induced by biotic stresses (Torres et al., 2002). Both AtRbohD and AtRbohF function in ROS-dependent abscisic acid signaling and stomatal closure (Kwak et al., 2003). More recently, AtRbohF was found to interact with Calmodulin 4 (CaM4) and is responsible for Receptor Protein Kinase 1 (RPK1)-triggered superoxide production and age-dependent cell death (Koo et al., 2017). A few group I WRKY TFs in tobacco were identified to be able to recognize and bind to the W-box *cis*-element in the promoter of *RbohB* and induce its expression in the immune response (Adachi et al., 2015). However, whether there is any non-group I AtWRKY modulating transcription of Rboh genes is largely unknown.

SA is a phytohormone originally proved to regulate innate immunity in plants (Dempsey et al., 2011). An early study showed that Isochorismate Synthase 1 (ICS1; also termed SA Induction-Deficient 2, SID2) is a crucial enzyme in the biosynthesis of SA (Wildermuth et al., 2001). More recently, two independent groups elucidated the last two steps in the isochorismate-derived SA biosynthetic pathway, in which the role of the cytosolic enzyme avrPphB susceptible 3 (PBS3) has been clarified (Rekhter et al., 2019; Torrens-Spence et al., 2019). SA has also been demonstrated in several studies to promote leaf senescence. First, SA content increases in an age-dependent manner during leaf development, causing the induction of some SAGs (Breeze et al., 2011; Morris et al., 2000; van der Graaff et al., 2006). Second, transgenic *Arabidopsis* overexpressing the SA-degrading salicylate hydroxylase gene *NahG* exhibits delayed leaf senescence (Lim et al., 2007; Morris et al., 2000). It has been documented that there exists crosstalk between ROS and SA in that hydrogen peroxide (H_2O_2) stimulates SA synthesis in tobacco and SA influences H_2O_2 production and H_2O_2-metabolizing enzymes (Leon et al., 1995; Rao et al., 1997). However, a more recent research indicates that SA accumulation is independent of H_2O_2, at least in *Arabidopsis* (Hieno et al., 2019). However, whether SA and H_2O_2 production is controlled by a single TF remains poorly understood.

Pseudomonas syringae is a bacterial pathogen infecting many plants, including *Arabidopsis* (Katagiri et al., 2002). A well-known phenomenon associated with pathogen challenge is the hypersensitive response (HR), which is often accompanied by accumulation of SA and by activated defense responses in the surrounding or even distal parts of the infected plants, leading to the development of systemic acquired resistance (Vlot et al., 2009). In *Arabidopsis*, some mutants with enhanced susceptibility to *P. syringae* have been isolated, among which a few were identified to be defective in SA biosynthesis, such as *eds1* (Aarts et al., 1998), *pad4* (Zhou et al., 1998), *sid2* (Wildermuth et al., 2001) and *eds5* (Nawrath et al., 2002). Thus, SA-mediated defense plays a vital role in limiting *P. syringae* growth.

We previously identified that multiple W-box elements were present in the promoter regions of *RbohD* and *ICS1* in *Arabidopsis*, suggesting that these two genes might be under the control of common or separate sets of WRKY TFs. A screening of the AtWRKY family through dual luciferase (LUC) reporter assay identified WRKY55 as a candidate. Moreover, *WRKY55* is induced by *Pst* DC3000 and SA treatments (Dong et al., 2003), suggesting a potential role of WRKY55 in several different processes. However, the role of WRKY55 in senescence and defense against pathogens and the underling mechanisms are not clear. We thus hypothesized that WRKY55 modulates ROS and SA levels and controls the relevant processes. Therefore, characterization of the WRKY55 subnetwork will be beneficial to our understanding of the complex crosstalk between senescence and defense against pathogens. In the present study, we report the identification of AtWRKY55 through a reverse genetic approach as a new factor that positively regulates leaf senescence and defense against *P. syringae*.

RESULTS

WRKY55 is predominantly expressed in senescing leaves

Among the 72 WRKY TF genes in *Arabidopsis*, the function of *WRKY55* has not yet been reported. WRKY55 contains 292 amino acids, with a single WRKY domain in the middle (Fig. 1A). A quantitative real-time PCR (qRT-PCR) profiling found that *WRKY55* was induced at an early stage of leaf senescence (ES), and its expression was further induced at a late stage of leaf senescence (LS) (Fig. 1B). An examination of a developmental map of *WRKY55* expression in different tissues or organs at the eFP browser website (Winter et al., 2007), based on the ATH1 microarray data of early years, also indicated that *WRKY55* is preferentially expressed in senescing leaves compared with young and mature leaves (Fig. S1). To examine the evolutionary relationships of WRKY55 in the WRKY family in *Arabidopsis*, we constructed a phylogenetic tree using a maximum parsimony algorithm after performing an alignment of amino acid sequences of WRKY domains of the 72 WRKY proteins. It can be seen that WRKY55 is clustered with WRKY46 and belongs to group III, which contains a total of 13 members (Fig. S2).

WRKY55 is a transcriptional activator and targeted to nuclei

To characterize the function of a WRKY TF, it is a prerequisite to know its ability to activate or repress transcription. To this end, we analyzed the ability of WRKY55 TF to activate reporter genes in budding yeast (*Saccharomyces cerevisiae*). Initially, the coding region of *WRKY55* was fused to the GAL4 DNA-binding domain (BD) to examine its ability to activate transcription from the GAL4 upstream activation sequence and thereby promote yeast growth. The yeast cells transformed with the pGBKT7-*WRKY55* plasmid or control pGBKT7 plasmid grew well on SD-WL (synthetic dropout medium without tryptophan and leucine) control medium, whereas on the selective SD-WLH (synthetic dropout medium without tryptophan, leucine and histidine) medium supplemented with 5 mM 3-AT (3-amino-1,2,4-triazole) or on SD-LWHA (synthetic dropout medium without tryptophan, leucine and adenine hemisulfate) medium, only yeast containing pGBKT7-*WRKY55* plasmid could grow (Fig. 1C). X-Gal staining assay of β-galactosidase activity also indicated strong staining. Therefore, WRKY55 protein has transcriptional activation activity, whereas the empty vector (EV) showed no transcriptional activation activity, as expected.

The *cis*-elements for many WRKY proteins have been identified, and it has been shown that W-box (TTGACC/T) is the consensus motif bound by WRKYs of many different groups (Ciolkowski et al., 2008). We therefore investigated whether WRKY55 binds to this *cis*-element through a dual LUC assay system. Quintuple tandem repeats of W-box sequences were inserted, together with the CaMV35S minimal promoter, upstream of firefly luciferase (fLUC) gene (Fig. 1D). The effector plasmid was pYJHA-*AtWRKY55*, with the control being pYJHA-*GFP*. The results showed that WRKY55 showed significant transactivation activity at the two time points examined (Fig. 1E).

Development (2020) 147, dev189647. doi:10.1242/dev.189647

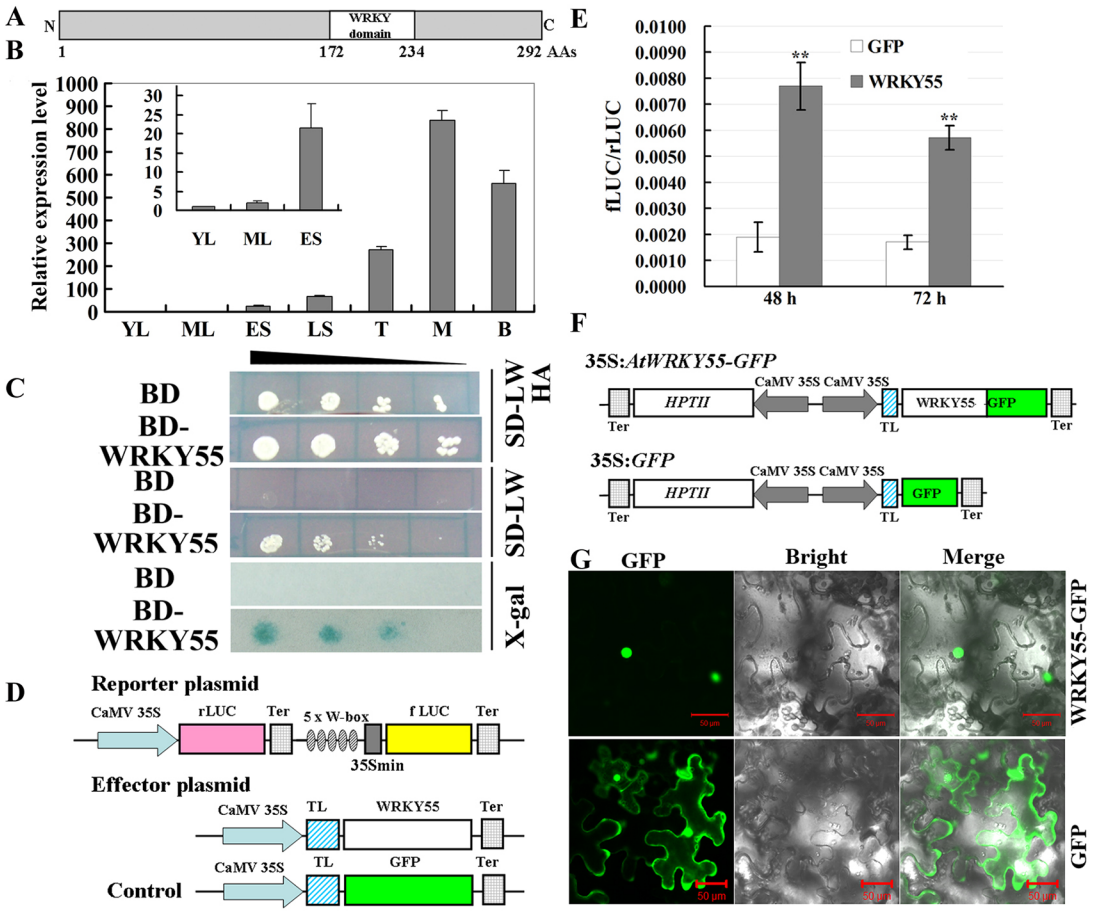

Fig. 1. Expression pattern, transactivational activity and subcellular localization of WRKY55. (A) Schematic representation of WRKY55 protein. A highly conserved WRKY domain responsible for DNA-binding (BD) ability is located in the middle. (B) qRT-PCR analysis of *AtWRKY55* expression during leaf senescence. ES, early senescent leaves at 35 dps; LS, late senescent leaves at 42 dps; ML, mature leaves at 28 dps; T, M and B indicate tip, middle and base of LS leaves; YL, young leaves at 21 dps. The transcript level of *WRKY55* in YL was set arbitrarily to be one. Data are the mean±s.e.m. of three biological replicates. (C) Transactivational activity assay in yeast. The yeast cells of strain AH109 harboring the indicated plasmids were grown on either the nonselective (SD-WL) or selective (SD-WLH+5 mM 3-AT and SD-LWHA) medium, followed by β-galactosidase assay (X-Gal staining). Decreasing cell densities in the dilution series are illustrated by narrowing triangles. BD represents empty pGBKT7 vector. (D) Schematic diagrams of effector and reporter constructs used in the dual luciferase assays. CaMV 35S promoter driving AtWRKY55 was used as the effector, and the GFP expression vector was used as a control. The dual luciferase reporter construct consists of 35S driving the *Renilla* luciferase (*rLUC*) reporter gene for internal normalization, and quintuple tandem W-box sequence driving the firefly luciferase (*fLUC*) reporter gene. Ter, terminatior sequence; TL, translational leader sequence. (E) AtWRKY55 showed transactivation activity in dual LUC assay. Data are the mean±s.e.m. of three biological replicates. Asterisks denote significant differences by Student's *t*-test (two-tailed, $^{**}P \leq 0.01$). (F) Schematic diagrams of T-DNA regions of constructs used in subcellular localization assay. *HPTII*, hygromycin resistance gene. (G) Subcellular localization of AtWRKY55 protein in *Nicotiana benthamiana* cells. The upper and lower panels represent WRKY55 and GFP alone, respectively. In each panel, the extreme left is GFP fluorescence, the middle bright field and the right an overlay of the two images as indicated on the top of the picture. Scale bars: 50 µm.

To determine the subcellular localization of WRKY55, a chimeric gene expression cassette containing a *WRKY55-GFP* fusion gene under the control of 35S promoter was expressed in leaves of *Nicotiana benthamiana* (Fig. 1F). We found that WRKY55-GFP signals were present in the nucleus only (Fig. 1G), which is in agreement with its role as a TF. As a control, we also examined the subcellular localization of the GFP protein in leaf cells, and green signals were present in both the cytosol and nuclei (Fig. 1G).

Overexpression of *WRKY55* induces ROS accumulation and precocious leaf senescence

In the aforementioned GFP subcellular assay in *N. benthamiana*, we also observed that expression of *WRKY55-GFP* in leaves led to hypersensitive response-like cell death within 2 days post-infiltration (dpi). To examine this, we performed 3,3′-diaminobenzidine (DAB) staining, showing production of ROS at the sites of infiltration (Fig. S3A). Further quantification of electrolyte leakage and H_2O_2 demonstrated a significant increase in ion leakage and H_2O_2 accumulation in leaf tissue expressing *WRKY55*, compared with the *GFP* control (Fig. S3B,C). Given that leaf senescence is a developmentally programmed cell death process and that overproduction of ROS could accelerate leaf senescence, we wanted to know whether overexpression of *WRKY55* in *Arabidopsis* could also lead to precocious leaf senescence. To this end, we generated an inducible overexpression (IOE) construct of *WRKY55*, based on an estradiol system (Zuo et al., 2000) and transformed it into wild-type (WT) *Arabidopsis*. In parallel, the *GUS* gene was also inducibly expressed in WT plants and used as the control. Through qRT-PCR, a few independent T3 transgenic lines showing high expression of *WRKY55* were obtained (Fig. S4A). At the seedling stage, the yellowing phenotype was very evident in four independent inducible lines of *WRKY55* (Fig. S5A). Similar to plants grown in soil mix in normal growth conditions, after treatment with β-estradiol (BE) an obvious yellowing of leaves was also observed on *WRKY55*-IOE

Development (2020) 147, dev189647. doi:10.1242/dev.189647

plants from 6 weeks post-stratification (wps), but not on the control (Fig. 2A). H_2O_2 is the most stable form of ROS, facilitating detection and quantification. Consequently, we performed DAB staining of the transgenic seedlings and identified obvious staining on the inducible overexpression lines, indicative of ROS accumulation (Fig. 3B). As the integrity of the plasma membrane of cells in tissues undergoing stresses or senescence is influenced, there is ion leakage, especially efflux of K^+ and other anions, which causes an increase in conductivity (Demidchik et al., 2014). We therefore quantified the physiological indicators and observed a significant decrease in chlorophyll and increase in H_2O_2 content and ion leakage with *WRKY55*-IOE plants compared with the control, especially at 7 wps (Fig. 2C-E). It was also noted that the difference was significant between the control *GUS*-IOE line and *WRKY55*-IOE lines for relative conductivity at 5 wps, which might be because the change in relative conductivity occurred earlier than that of chlorophyll and H_2O_2 contents.

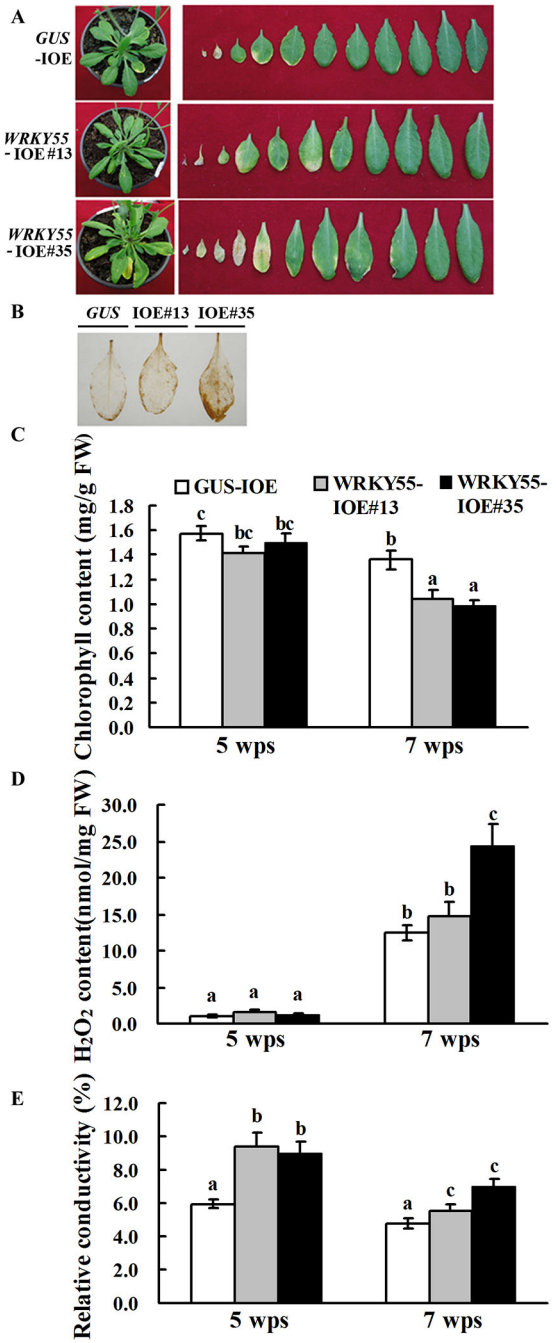

Fig. 2. Inducible overexpression of *WRKY55* promoted leaf senescence. (A) Comparison of leaf senescence phenotype of transgenic lines expressing *GUS* or *AtWRKY55* at 6 wps. Rosette leaves were excised from age-matched plants and arranged from the oldest to the youngest. The picture was taken 1 week after spraying with 5 µM BE. (B) DAB staining of the eighth rosette leaves of transgenic plants at 6 wps. (C-E) Quantification of chlorophyll (C) and hydrogen peroxide (D) contents and ion leakage (E) in the fifth to eighth rosette leaves of different genotypes. Values represent the mean±s.e.m. of three independent assays for each time point. Different letters indicate significant differences by one-way ANOVA (P<0.05).

Transfer DNA insertion mutants of *WRKY55* show delayed leaf senescence

To gain a better understanding of the role of *WRKY55* in leaf senescence, we obtained two transfer DNA (T-DNA) insertion mutants and identified homozygous lines through PCR. Sequencing of the flanking sequences showed that SALK_119078 (*wrky55*-1) and GABI_171G05 (*wrky55*-2) lines have the T-DNA inserted in the first intron (Fig. 3A). Specifically, *wrky55-1* harbors a T-DNA insertion between the first and second nucleotide of the first intron, which is expected to interfere with the splicing of this intron, whereas T-DNA was inserted near the 3′ end of the first intron in *wrky55-2*. RT-PCR analysis using primers targeted to the third exon showed that *WRKY55* transcripts were not detectable in *wrky55-1*, whereas a significant decrease was observed in the *wrky55-2* mutant (Fig. 3B), suggesting that *wrky55-1* is a loss-of-function mutant, whereas *wrky55-2* might be a knockdown mutant.

In normal conditions and at the seedling stage, the two mutants did not show much difference from the WT on half-strength Murashige and Skoog (MS) medium (Fig. S5B). When grown in soil mix, the two *wrky55* mutants showed delayed leaf senescence compared with the WT plants from 7 wps (Fig. 3C). We examined and compared a few physiological indicators between mutants and WT control. The contents of chlorophyll in rosette leaves of the two mutants did not show any significant difference from that of the WT at 4 wps. At 7 wps, chlorophyll concentrations in rosette leaves of *wrky55* mutants were significantly higher than that in the age-matched WT plants (Fig. 3D), which is consistent with a delayed leaf-yellowing phenotype in the two mutants. The two *wrky55* mutants had a lower level of H_2O_2 than that in WT at 7 wps, although in plants of 4 wps, no significant difference was observed (Fig. 3E). With respect to ion leakage, there was no significant difference between mutants and WT at 4 wps, but electrolyte leakage in *wrky55* mutants was less than that in WT at 7 wps (Fig. 3F). These data support that mutation of *WRKY55* delays leaf senescence.

Constitutive overexpression of *WRKY55* induces premature leaf senescence

To confirm the potential involvement of *WRKY55* in the positive regulation of leaf senescence, we also constitutively overexpressed (COE) it using the cauliflower mosaic virus (CaMV) 35S promoter. As a control, the *GFP* gene was also expressed on the background of WT Col-0 ecotype under the same promoter. A qRT-PCR assay of multiple lines transformed with 35S:*WRKY55* showed elevated *WRKY55* transcript levels in a few independent transformants (Fig. S4B). A phenotypic comparison of the different genotypes demonstrated that two *WRKY55*-COE lines also showed accelerated leaf senescence, compared with the *GFP*-expressing control (Fig. 4A). We also monitored the contents of chlorophyll and H_2O_2 and found that the chlorophyll content was significantly lower in the two *WRKY55*-COE lines than in the control at 7 wps, although

Development (2020) 147, dev189647. doi:10.1242/dev.189647

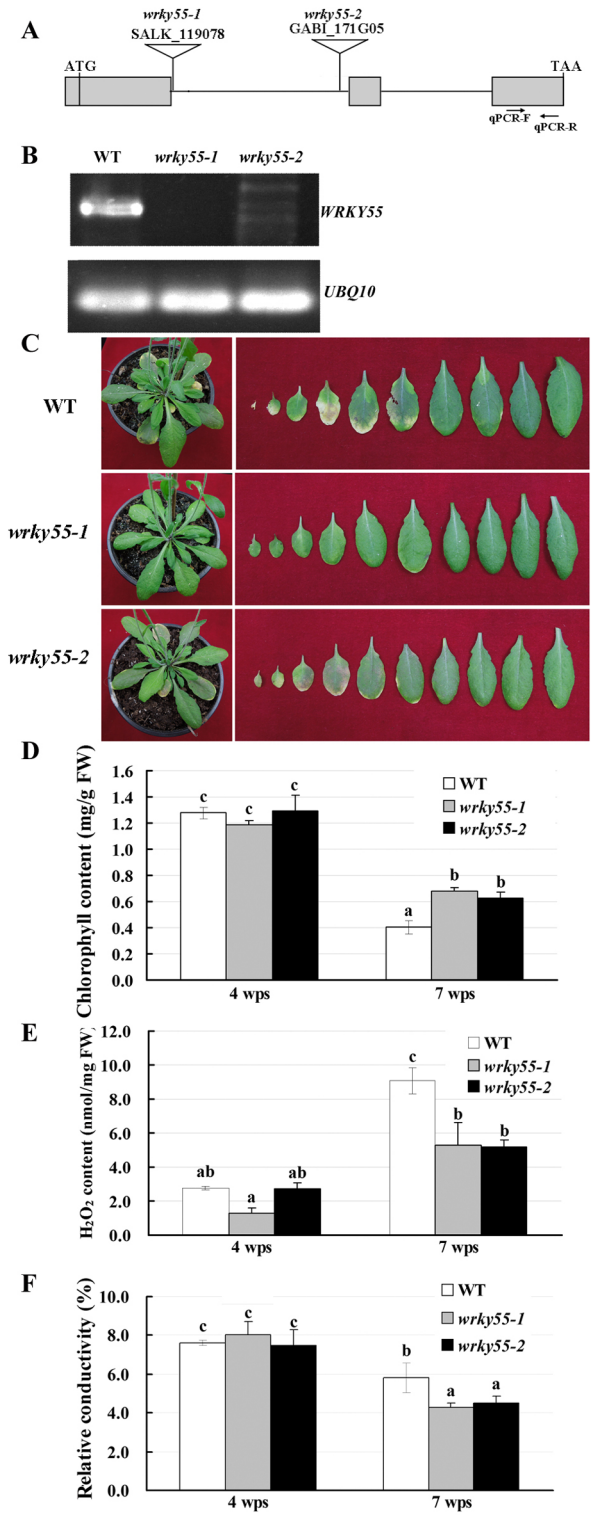

Fig. 3. Phenotypic assay of mutant lines and measurement of physiological indexes. (A) Gene structure of *AtWRKY55* and locations of T-DNA inserts. Rectangles represent exons and lines denote introns. (B) RT-PCR analysis of *AtWRKY55* expression in seedlings of WT and two mutants. *UBQ10* was amplified as the endogenous control. (C) Comparison of leaf senescence phenotypes between WT and mutants at 7 wps. Rosette leaves were excised from age-matched plants and arranged from the oldest to the youngest. (D-F) Quantification of chlorophyll (D) and hydrogen peroxide (E) contents and ion leakage (F) in the fifth to eighth rosette leaves of different genotypes. Values represent the mean±s.e.m. of three independent assays for each time point. Different letters indicate significant differences by one-way ANOVA (P<0.05).

no significant difference was observed at 4 wps (Fig. 4B). By contrast, the H_2O_2 content in the two *WRKY55*-COE lines was a little higher than the control at 4 wps, and the content of H_2O_2 was significantly higher in the two *WRKY55*-COE lines than in the *GFP* control at 7 wps (Fig. 4C). Collectively, these data reveal a role of WRKY55 in the control of developmental leaf senescence.

Transcriptome profiling identifies differentially expressed genes regulated by WRKY55

Next, to identify the target genes of WRKY55, we conducted RNA-sequencing (RNA-seq) analysis of *WRKY55*-IOE#13 compared with transgenic *GUS*-IOE plants after induction by BE for 2 days. A total of 1448 differentially expressed genes (DEGs) between *WRKY55*-IOE#13 and *GUS*-IOE plants were identified using a cut-off of 2-fold ($|\log_2$ fold change$|\geq 1$ and P-value <0.05). Among the DEGs, 1157 genes were upregulated, whereas 291 genes were downregulated in the *WRKY55*-IOE#13 compared with *GUS*-IOE (Fig. 5A). Given that our results indicated that WRKY55 is a transcriptional activator, we were more interested in the upregulated genes. Gene ontology (GO) enrichment analysis revealed that three

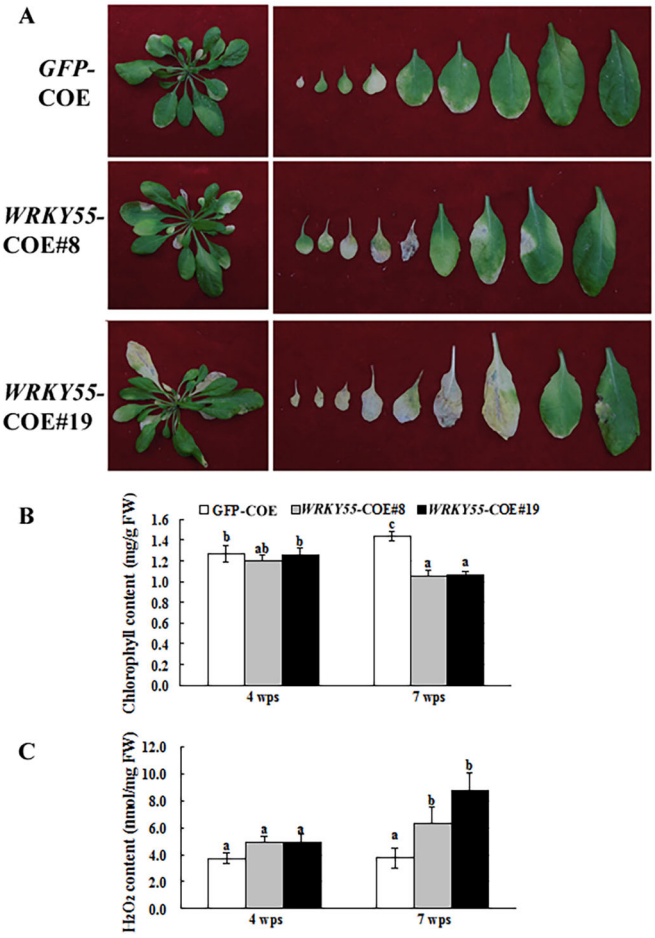

Fig. 4. Constitutive overexpression of *WRKY55* causes precocious senescence. (A) Comparison of leaf senescence phenotypes between *GFP*-expressing and two *WRKY55*-overexpressing lines at 7 wps. Right panels show rosette leaves excised from age-matched plants and arranged from the oldest to the youngest. (B,C) Quantification of chlorophyll (B) and H_2O_2 (C) contents in the fifth to eighth rosette leaves of different genotypes. Values represent the mean±s.e.m. of three independent assays for each time point. Different letters indicate significant differences by one-way ANOVA (P<0.05).

Development (2020) 147, dev189647. doi:10.1242/dev.189647

groups of genes are prominent among the upregulated DEGs. The first group of genes is implicated in ROS biosyntheses, including *RbohA*, *RbohD* and *RbohI* (Torres and Dangl, 2005). The second group is composed of genes responsible for SA biosynthesis and signaling, i.e. *ICS1*, *PBS3*, *NPR2*, *Pathogenesis-Related 1* (*PR1*), *PR5* and *SARD1* (Zhang and Li, 2019). The third group comprises well-known positive regulators or marker genes of leaf senescence, which include *SAG13*, *SAG29* (*SWEET15*), *WRKY75* and *MYB2* (Woo et al., 2019) (Fig. 5B). We did not identify any genes encoding proteins implicated in chlorophyll catabolism or degradation (Ren et al., 2007) among the upregulated genes.

WRKY55 transactivates the expression of a few functional genes

Considering that WRKY55 is a transcriptional activator, we next sought to establish the connection between WRKY55 and putative target genes. In particular, we investigated whether WRKY55 transcriptionally activates any of the upregulated functional genes. Therefore, we performed a dual LUC-based transactivation assay. Promoters were individually fused with the *fLUC* reporter gene and served as reporter constructs. Each reporter construct contains a separate expression cassette, in which *rLUC* is driven by CaMV 35S promoter and functions as an internal control (Fig. 6A). A construct harboring 35S:*WRKY55* was used as the effector, and 35S:*GFP* was included as a control. To monitor the transcriptional regulation, samples at two time points (2 and 3 days) were assayed. The results demonstrated that expression of *WRKY55* significantly transactivated the expression of *fLUC* driven by *RbohD*, *ICS1*, *PBS3* and *SAG13* promoters, compared with the *GFP* control (Fig. 6B). In addition, activities of *RbohA* and *SAG29* promoters were also significantly increased by WRKY55, with a relatively higher fLUC:rLUC ratio compared with that of the GFP control

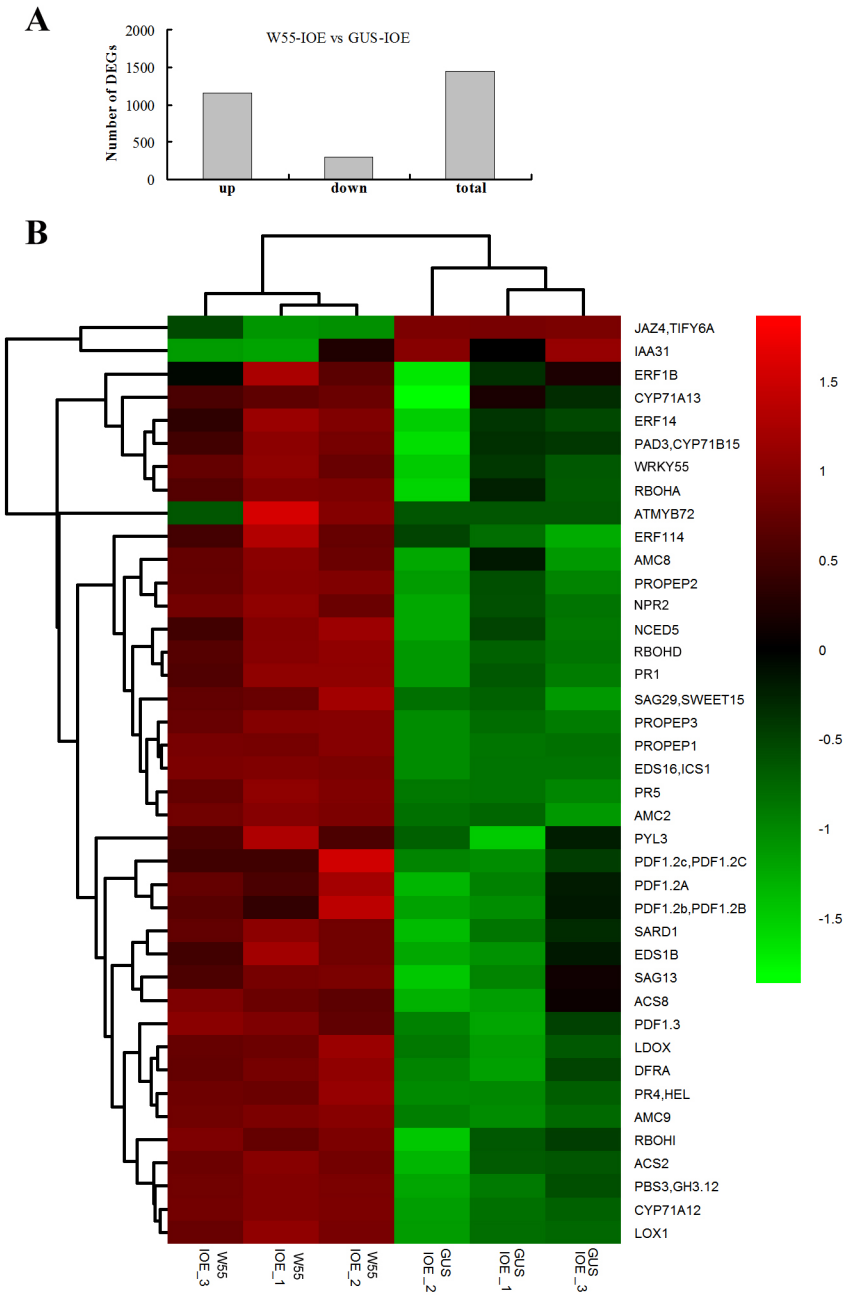

Fig. 5. Heat map illustration of representative differentially expressed genes between inducible *WRKY55* line and *GUS* control line by RNA sequencing. (A) Counting of DEGs from RNA-seq analysis between *WRKY55*-IOE and *GUS*-IOE control. (B) Cluster heat map analysis of representative DEGs between *WRKY55*-IOE and *GUS*-IOE control. The expressions of DEGs are hierarchically clustered on the *y*-axis, and six samples (three biological replicates) are hierarchically clustered on the *x*-axis. The values of DEGs in the six samples are normalized by a scale function. The up- and downregulated genes are presented in red and green, respectively.

Development (2020) 147, dev189647. doi:10.1242/dev.189647

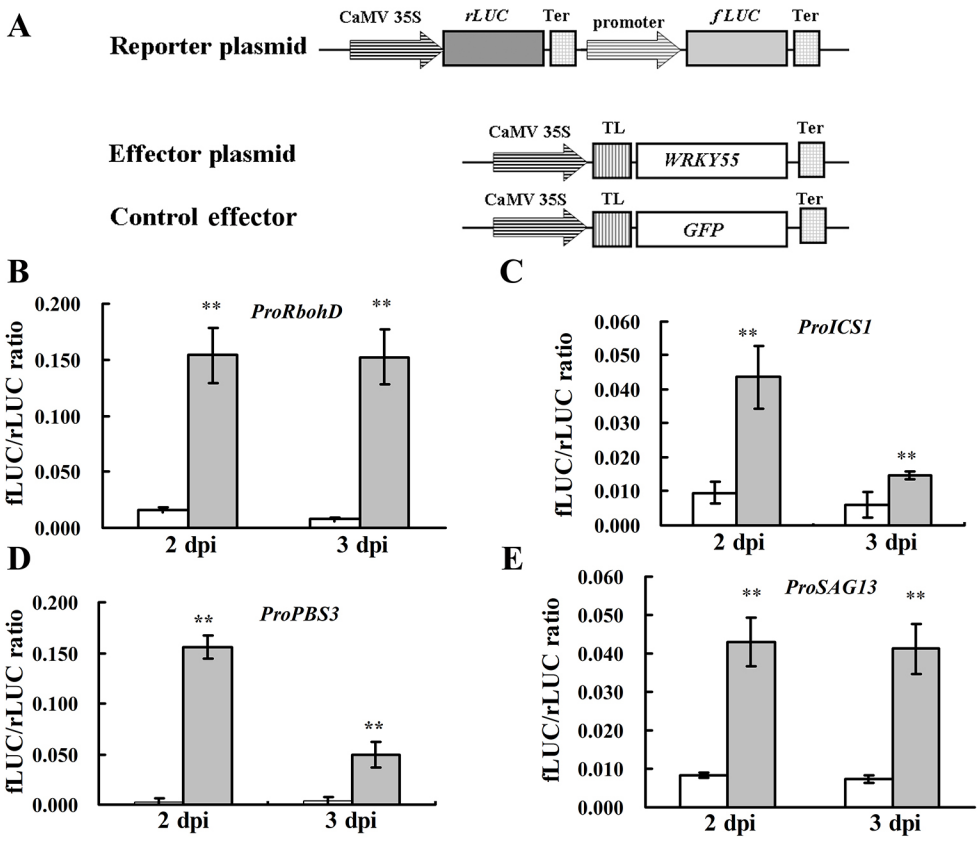

Fig. 6. Assay of transcriptional regulation of WRKY55 through dual LUC reporter assay. (A) Schemes of the plasmids used. The reporter plasmid contains the respective promoter regions fused to *fLUC* and the *Renilla* luciferase (*rLUC*) gene driven by CaMV35S. The effector plasmid contains the *WRKY55* driven by the CaMV 35S. The *GFP*-expressing plasmid was used as a negative effector control.
(B-E) Transactivation assay of different promoters by WRKY55. Relative LUC activity was represented by the ratio of fLUC to rLUC. Error bars indicate the s.e.m. of three biological replicates. Asterisks denote significant differences by Student's *t*-test (two-tailed, $^{**}P \leq 0.01$).

(Fig. S6). However, expression of *WRKY55* significantly repressed or did not change the *fLUC* expression under the control of *RbohB*, *RbohI*, *ICS2*, *EDS5*, *SAG12* and *PR1* promoters (Fig. S6B).

Furthermore, to test whether the expression levels of the genes of interest were decreased in *wrky55* mutants compared with WT, we used qRT-PCR. The results showed that *ICS1*, *PBS3*, *RbohD* and *SAG13* were significantly downregulated in the knockout *wrky55-1* mutant compared with WT (Fig. 7A). However, the expression of *RbohA* and *SAG29* did not show evident decrease or even increased slightly, suggesting that these two genes are indirect targets of WRKY55 or are also regulated by other unknown TFs.

WRKY55 positively regulates the accumulation of SA and the defense response

Considering the fact that RNA-seq analysis identified several genes for rate-limiting steps of SA biosynthesis, we measured the contents

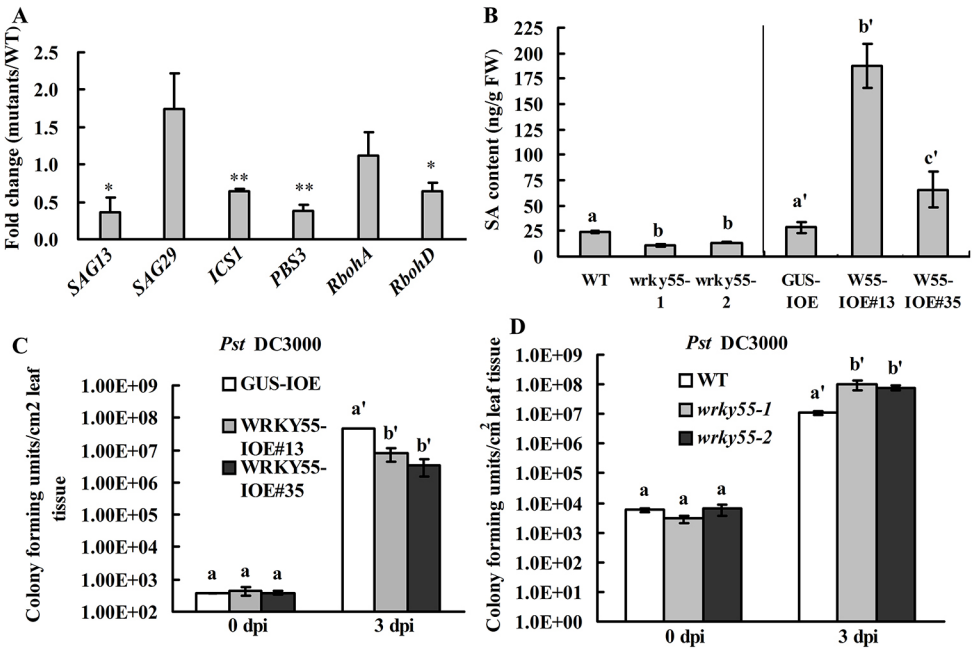

Fig. 7. qRT-PCR, SA quantification and bacterial pathogen assays. (A) qRT-PCR analysis of expression levels of putative target genes in *wrky55-1* mutant compared with WT. Each value represents the mean±s.e.m. of three biological replicates. The *UBQ10* and *UBC21* mRNA levels were used as the endogenous control. Asterisks denote significant differences (compared with one) by Student's *t*-test (two-tailed, $^{*}P \leq 0.05$, $^{**}P \leq 0.01$). (B) Measurements of free SA in *WRKY55*-related materials with individual controls. Values are mean±s.e.m. of four biological replicates. (C) Inducible overepxression of *WRKY55* caused decreased susceptibility to *Pst* DC3000. (D) Mutations of *WRKY55* caused susceptibility to *Pst* DC3000. In both C and D, bacterial growth was analyzed at 0 and 3 dpi. The bars represent mean±s.e.m. of three biological replicates. Different letters indicate significant differences by one-way ANOVA ($P<0.05$).

Development (2020) 147, dev189647. doi:10.1242/dev.189647

of SA in *WRKY55*-IOE and mutant lines and in the corresponding control lines. The results showed that the free SA contents in the two *wrky55* mutants were significantly lower than those of WT control (Fig. 7B). By contrast, the free SA contents in the leaves of *WRKY55*-IOE#13 and *WRKY55*-IOE#35 lines were 7- and 2.8-fold higher than that of the *GUS*-IOE line, respectively (Fig. 7B). These data suggest that, besides inducing ROS accumulation, WRKY55 positively regulates SA accumulation.

Considering that ROS and SA contents are stimulated upon infection by many pathogens and that reduced ROS and SA levels increase susceptibility to bacterial pathogens (O'Brien et al., 2012; Zhang and Li, 2019), we performed a bacterial growth assay against pathogenic bacteria *P. syringae* pv. *tomato* DC3000 (*Pst* DC3000). Upon inoculation with *Pst* DC3000 for 3 days, in the infiltrated rosette leaves of mature plants, less bacterial growth was observed in *WRKY55-IOE* plants compared with the transgenic *GUS* control, after induction by BE, whereas no significant difference was observed among the three lines at 0 dpi (Fig. 7C). By contrast, more bacterial growth was observed in *wrky55-1* and *wrky55-2* mutants compared with the WT control at 3 dpi, and no difference was observed at 0 dpi (Fig. 7D). Collectively, these data indicate that WRKY55 positively regulates resistance to *Pst* DC3000.

WRKY55 binds directly to the promoters of target genes via W-box

We also surveyed the promoters of *RbohD*, *ICS1*, *PBS3* and *SAG13* and identified the presence of five, four, five and one W-box [TTGAC(C/T)], respectively (Fig. 8; Fig. S7). To determine the binding, we purified WRKY55 protein fused to the glutathione *S*-transferase (GST) tag from *Escherichia coli* and used a biotin labeling method to label the probes, which were used for electrophoretic mobility shift assay (EMSA). First, we tested the

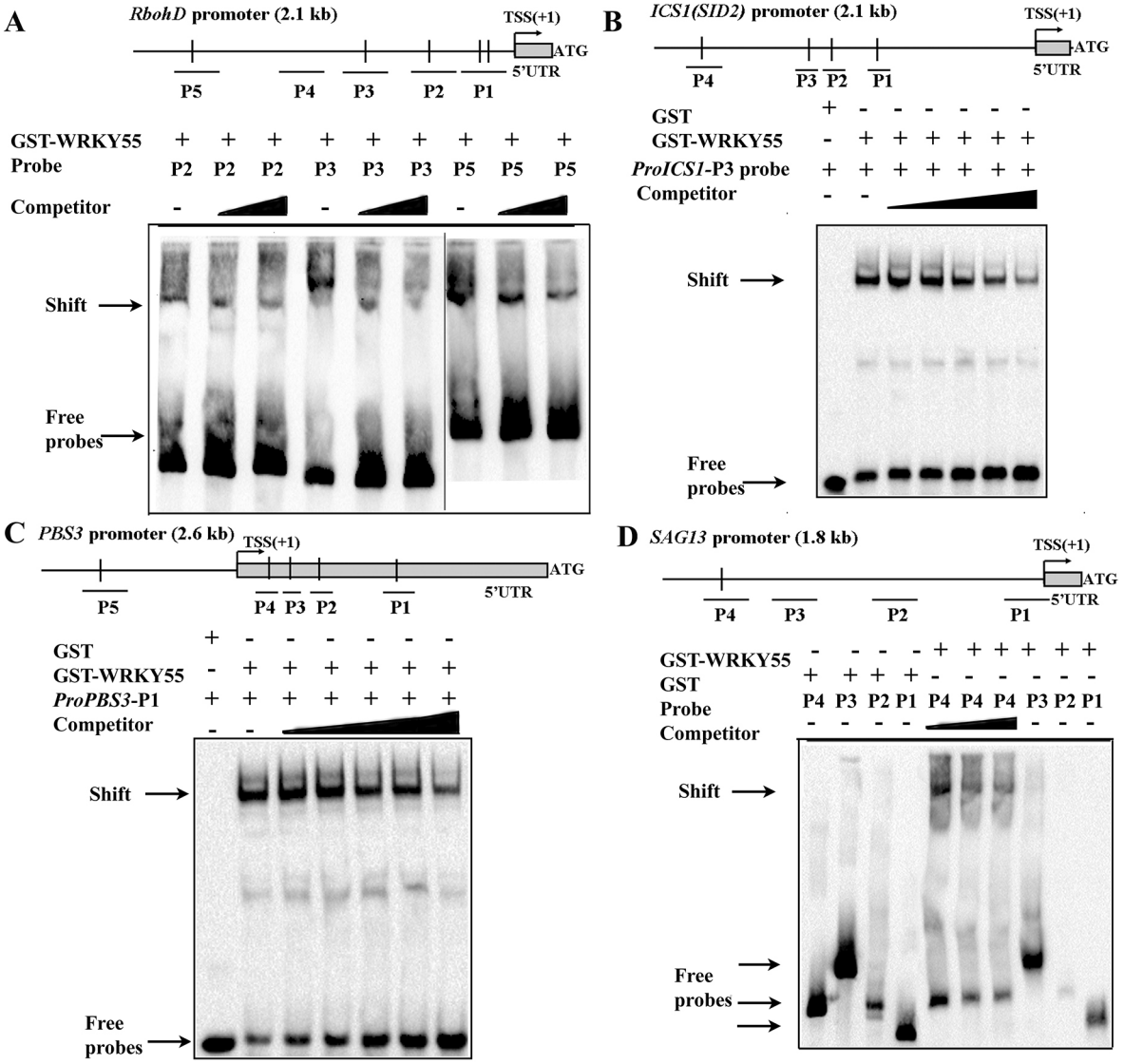

Fig. 8. Electrophoretic mobility shift assay of WRKY55 binding to different fragments of target genes. Binding of GST-WRKY55 to different fragments with or without the W-box element in promoters (including the 5′ UTR) *RbohD* (A), *ICS1* (B), *PBS3* (C) and *SAG13* (D) was tested. In the upper part of each panel is a schematic diagram of the promoter and W-box elements (shown by vertical lines). Arrows denote the transcription start site (TSS). ATG is the translational initiation codon. Gray rectangles indicate the 5′ UTR. P1 to P4 or P5 represent the fragments labeled with biotin and used as probes. GST protein was used as a negative control. A few fragments that harbor only W-box-like elements were also tested in parallel. Black triangles indicate increasing amounts of competitive probes. –, absence; +, presence. The arrows at the upper and lower parts of the membrane show DNA-protein complexes (shift) and free probes, respectively.

Development (2020) 147, dev189647. doi:10.1242/dev.189647

binding of WRKY55 to quadruple tandem repeats of W-box and mutated sequences, in which a single mutation was made. The results confirmed that the GST-WRKY55 fusion protein bound to the WT W-box probe and caused a clear shift, but not to the mutated W-box (mW-box) probe, in which TTGAC(C/T) was mutated to TTGAA(C/T) (Fig. S8). By contrast, GST alone failed to bind to either WT or mutated W-box element (Fig. S8). Second, the binding of GST-WRKY55 to W-box-containing fragments in the individual promoters was tested. The results showed that WRKY55 bound obviously to the P2, P3 and P5 probes (Fig. 8A), but no significant binding to P1 or P4 fragments was detected (Fig. S9). As expected, the GST protein was not able to bind to any of the five fragments (Fig. S9). A competitive binding assay with excessive cold probes indicated that binding of WRKY55 to the labeled P2, P3 and P5 fragments was inhibited by an excess of unlabeled probes (Fig. 8A). With respect to *ICS1* promoter, an initial screening of binding showed that WRKY55 bound to P3 probe among the four probes examined (Fig. S10), and this binding could be competed with by excessive cold probes (Fig. 8B). For *PBS3* promoter, an initial screening of binding showed that WRKY55 bound to P1, P2 and P4 probes, but not to the P3 probe (Fig. S11), and the binding was successfully competed for by excessive cold probes (Fig. 8C; Fig. S12). Finally, WRKY55 bound to the W-box-containing P4 segment of the *SAG13* promoter, but not to P1-P3 segments, which contain only W-box-like elements (Fig. 8D). Moreover, an excessive amount of unlabeled competitive probes of P4 effectively competed with the binding (Fig. 8D).

We next used chromatin immunoprecipitation (ChIP) to test the binding of WRKY55 to its target gene promoters *in vivo*. For this assay, inducible *WRKY55*-HA seedlings were used, with the inducible *GUS*-HA line as the control. Chromatins were pulled down through an anti-HA antibody, with abundance compared between these two different transgenic lines. Primers for each of the putative binding sites were designed to flank promoter regions that contain W-box elements (Fig. 9A). The results revealed that WRKY55 significantly enriched the fragments containing F1 and F2 of *ProRbohD* (Fig. 9B), F2 and F3 of *ProICS1* (Fig. 9C), F1-F3 of *ProPBS3* (Fig. 9D) and F1 of *ProSAG13* (Fig. 9E), whereas WRKY55 did not show any enrichment of individual controls of these genes. The minor difference between *in vitro* EMSA and *in vivo* ChIP-qPCR might be caused by the two experimental systems. Overall, these assays indicated that WRKY55 can bind directly to the promoters of *RbohD*, *ICS1*, *PBS3* and *SAG13* via the W-box element.

Mutation of *ICS1* partly suppresses the early leaf senescence phenotype of *WRKY55*-overexpressing plants

Given that the above data indicate that two key genes implicated in SA synthesis are targets of WRKY55, we decided to examine the

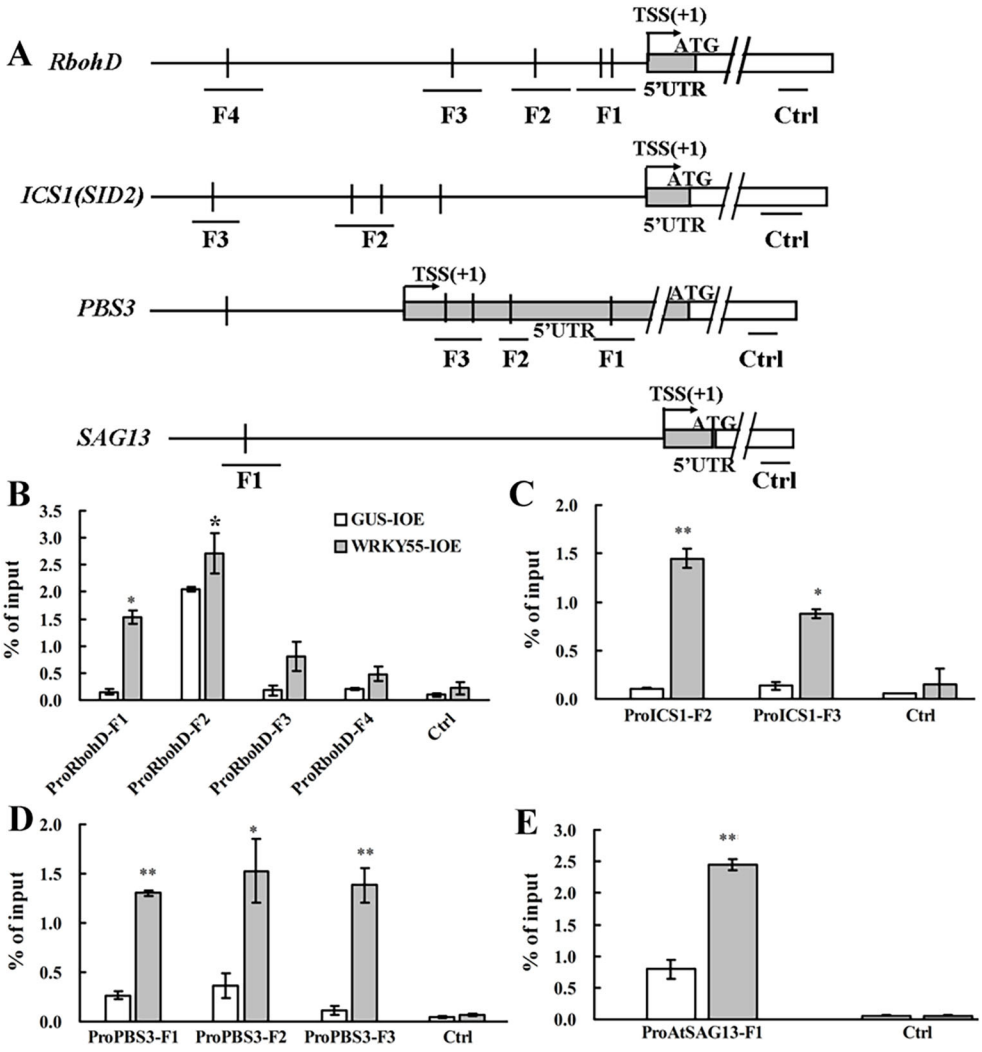

Fig. 9. ChIP-qPCR assay to confirm the binding of WRKY55 to its target gene promoters. (A) Schematic diagrams of W-box elements and primer location in promoter regions of *RbohD*, *ICS1*, *PBS3* and *SAG13* genes, with control primers indicated by Ctrl. TSS, transcription start site. ATG represents the translational initiation codon. Gray and white rectangles represent the 5′ UTR and coding regions, respectively. The lines below W-boxes (indicated with vertical lines) and Ctrl indicate the sequences detected in ChIP-qPCR assay. (B-E) Association of WRKY55 with its targets by ChIP-qPCR assay. Chromatin was prepared from 14-day-old *WRKY55*-IOE or *GUS*-IOE (control) plants, using anti-HA antibody, followed by detection by qPCR. Enrichment of specific fragments is expressed as a percentage of input. Data are mean±s.e.m. of three biological replicates. Statistical analysis was performed with Student's *t*-test (two-tailed, $*P<0.05$, $**P<0.01$).

Development (2020) 147, dev189647. doi:10.1242/dev.189647

genetic relationship. As a crucial enzyme involved in SA synthesis (Wildermuth et al., 2001), ICS1 (also called SID2) was selected, because it has been used as the background for genetic analyses in previous studies (Chen et al., 2009; Guo et al., 2017). We therefore crossed *WRKY55*-IOE#13 with the *sid2-2* mutant to generate *WRKY55*-IOE#13*/sid2-2* plants. In normal long-day growth conditions, *WRKY55*-IOE#13*/sid2-2* plants showed a delayed senescence phenotype compared with *WRKY55*-IOE#13 plants after induction by BE (Fig. 10A). Accordingly, a higher content of chlorophyll and lower relative conductivity also indicated the delayed senescence phenotype in *WRKY55*-IOE#13*/sid2-2* plants (Fig. 10B,C). Collectively, these data suggest that *ICS1* is epistatic to *WRKY55*.

DISCUSSION

Leaf senescence is the last stage of leaf development and is characterized by loss of chlorophylls and massive programmed cell death (Woo et al., 2019). Leaf senescence is important for fitness in adverse conditions, because it enables relocation of essential nutrients from aging leaves to developing tissues and sink (Woo et al., 2013). Leaf senescence is also a type of developmentally programmed cell death, which is, to some extent, similar to hypersensitive response-like cell death in the defense response (Daneva et al., 2016). Previous research has demonstrated that leaf senescence is regulated not only by endogenous signals, such as age and hormones, but also by many environmental stressors (Lim et al., 2007; Woo et al., 2019). Some SAGs that are upregulated during senescence have been identified, and the encoded proteins are diverse (Gan and Amasino, 1997; Guo et al., 2004). For instance, *AtSAG12* encodes a cysteine protease involved in nitrogen mobilization during senescence (James et al., 2018); *AtSAG13* encodes a short-chain alcohol dehydrogenase (Weaver et al., 1998); *AtSAG29* encodes a sugar transporter belonging to the SWEET family (Seo et al., 2011); and *AtSAG113* encodes a protein phosphatase type 2C family member specifically suppressing stomatal closure (Zhang et al., 2012). Besides, many upstream regulators regulating diverse SAGs and/or other functional genes have also been identified through loss-of-function and/or gain-of-function studies in model plants, such as *Arabidopsis* and rice (Lim et al., 2007; Woo et al., 2013, 2019). Among these upstream regulators, TFs are interesting candidates because they could affect the expression of an array of genes, including SAGs, and thus act as inducers or brakes of the senescing transcriptome. It should be noted that leaf senescence at the late stage of development is irreversible, which means that a regulator can accelerate or delay the progression of leaf senescence but ultimately cannot prevent it from happening. Members of the WRKY and NAC families are prominent among the reported transcriptional regulators of leaf senescence, which include both positive and negative regulators. For example, WRKY6 and WRKY53 regulate leaf senescence positively through different sets of targets (Miao et al., 2004; Robatzek and Somssich, 2001). WRKY45 directly binds the promoters of several SAGs, such as *SAG12*, *SAG13*, *SAG113* and *SEN4*, to regulate age-triggered leaf senescence positively (Chen et al., 2017). WRKY57 directly represses the expression of *SEN4* and *SAG12* in JA-induced leaf senescence (Jiang et al., 2014). WRKY75 positively regulates leaf senescence by enhancing SA synthesis and repressing ROS degradation (Guo et al., 2017). By contrast, WRKY54 and WRKY70 cooperate as negative regulators during leaf senescence (Besseau et al., 2012). However, the exact target genes of some of these WRKY TFs are not yet clear. Besides, this evidence indicates that WRKY TFs could act to shorten or extend the lifespan of plants, depending on their target genes. Moreover, although genes of the WRKY family constitute the second largest group among all TF families in previous senescence transcriptome investigations (Guo et al., 2004; Woo et al., 2016), the functions and mechanisms of the majority of WRKY family members induced during the progress of leaf senescence remain elusive.

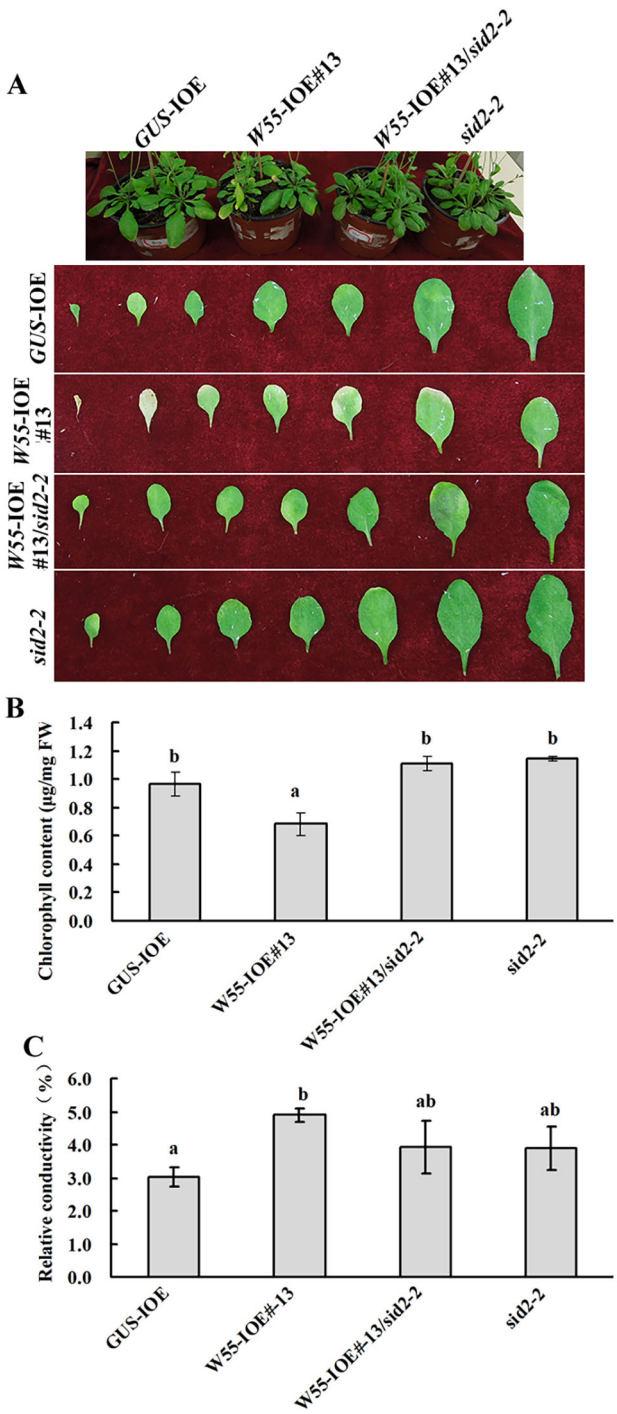

Fig. 10. Knockout mutation of *SID2* partly suppresses the early senescence phenotype of *WRKY55*-overexpressing plants. (A) Leaf senescence phenotype of 42-day-old *GUS*-IOE, *WRKY55*-IOE#13, *WRKY55*-IOE#13/*sid2-2* and *sid2-2* plants. (B,C) Measurements of chlorophyll contents (B) and relative conductivity (C) in the fifth to eighth rosette leaves. Data are mean±s.e.m. of three to four independent biological replicates. Identical and different letters represent nonsignificant and significant differences (P<0.05, one-way ANOVA).

Development (2020) 147, dev189647. doi:10.1242/dev.189647

In the present study, we showed that WRKY55 positively regulates age-dependent leaf senescence and bacterial pathogen resistance through both ROS and SA pathways. Our research showed that *WRKY55* expression is highly induced in senescent leaves compared with young and mature leaves (Fig. 1), suggesting that WRKY55 acts as an SAG. To examine the function of *WRKY55*, phenotypes of relevant transgenic lines were investigated. Loss-of-function *wrky55* mutants show delayed leaf senescence, whereas both constitutive and inducible *WRKY55*-overexpressing plants accelerated leaf senescence compared with respective control plants (Figs 2-4). These data support that WRKY55 plays a central role in controlling leaf senescence. By using a transgenic line in which *WRKY55* expression is induced with BE, we revealed many different genes that are upregulated by WRKY55 via an RNA-seq analysis (Fig. 5). Notably, a portion of the upregulated genes were previously identified to be induced during leaf senescence (Breeze et al., 2011; Buchanan-Wollaston et al., 2005; Guo et al., 2004; Woo et al., 2016). A transcriptional activation assay indicates that WRKY55 can regulate the expression of *RbohD*, *ICS1*, *PBS3* and *SAG13* (Fig. 6), and these four genes also exhibit opposite expression patterns in *wrky55* mutant plants (Fig. 7A). A few other interesting genes were excluded from further analysis because they failed to show opposite expression profiles, suggesting that other WRKY TFs (e.g. the close paralog, WRKY46; Fig. S1) might also regulate these genes and that they (WRKY55 and WRKY46) might be functionally redundant. Consistent with the changes in expression of several *Rboh* genes and *ICS1* and *PBS3*, the levels of H_2O_2 and free SA are decreased in mutants of *wrky55* and increased in *WRKY55*-overexpressing plants (Figs 2D, 3E, 4C and 7B).

It is well known that ROS (especially H_2O_2) and SA are signaling molecules that play important roles in many processes, such as stress responses and senescence (Baxter et al., 2014; Rivas-San Vicente and Plasencia, 2011). The extracellular ROS generated by plasma membrane-localized Rbohs can act as antimicrobials, cross-linkers of the cell wall to block pathogen invasion, or local and systemic secondary messengers to trigger relevant immune responses (Suzuki et al., 2011). In *Arabidopsis*, it is reported that the NADPH oxidase responsible for the pathogen-associated molecular patterns (PAMP)-induced ROS burst is RbohD (Nühse et al., 2007). SA, as a phytohormone, plays a crucial role in resistance against biotrophic pathogens (Vlot et al., 2009). An early study showed that SA levels increase ∼4-fold at the mid-senescent stage in *Arabidopsis*, and expression of several SAGs, such as *SAG12*, are considerably reduced in SA-deficient *NahG* transgenic *Arabidopsis* plants (Morris et al., 2000). Moreover, another gene expression analysis in *Arabidopsis* senescent leaves indicated that ∼20% of the upregulated genes during senescence show ≥2-fold reduced expression in SA-deficient *NahG* transgenic plants (Buchanan-Wollaston et al., 2005). However, how ROS and SA signals are integrated to determine the onset and progression of senescence and defense activation remains to be unraveled. More recently, ANAC017, ANAC082 and ANAC090 were reported to constitute a troika that negatively regulates leaf senescence at presenescent stages by inhibiting ROS and SA pathways (Kim et al., 2018). Nevertheless, these three NAC TFs were identified to regulate the expression of mostly signaling genes and other TF genes involved in ROS and SA responses (Kim et al., 2018), suggesting the existence of other TFs positively modulating the levels of ROS and SA.

In this study, we identified that WRKY55 can positively regulate the transcription of genes responsible for the biosynthesis of both ROS and SA, which positively control the progression of leaf senescence and defense against a bacterial pathogen. In this meaning, two different processes are under the control of ROS and SA at the same time, in which WRKY55 acts as a master regulator. Accordingly, *wrky55* plants show enhanced susceptibility, whereas *WRKY55*-overexpressing plants exhibit increased resistance to a virulent strain of the bacterial pathogen *Pst* DC3000 as measured in bacterial growth compared with control plants (Fig. 7C,D). Furthermore, through *in vitro* EMSA and *in vivo* ChIP-qPCR assays, we identified that it is the W-box elements in the promoters of *RbohD*, *ICS1*, *PBS3* and *SAG13* that mediate their induction by WRKY55 (Figs 8 and 9). A genetic analysis also demonstrated that mutation in *ICS1* can partly rescue the early senescence phenotype of *WRKY55*-overexpressing plants (Fig. 10). Compared with WRKY53, which is a well-characterized regulator of senescence in *Arabidopsis* and a convergence node of the SA and JA signaling pathways (Miao et al., 2004; Miao and Zentgraf, 2007), WRKY55 seems different in that it also regulates ROS biogenesis. Concerning the regulatory mechanism, WRKY55 is also different from other reported positive regulators of leaf senescence, including WRKY6, WRKY45, WRKY75 (Chen et al., 2017; Guo et al., 2017; Robatzek and Somssich, 2001, 2002; Zhang et al., 2017) and several members of the NAC family (Kim et al., 2016). Therefore, we conclude that *WRKY55* offers a good candidate for us to investigate the underlying mechanisms implicated in leaf senescence and pathogen resistance. This knowledge will be instrumental for us to design a better strategy of breeding crops with an optimal growth rate and effective immunity against pathogens.

In summary, this study shows that *Arabidopsis* WRKY55 acts a transcriptional activator and positively regulates leaf senescence and resistance against a bacterial pathogen, *Pst* DC3000. We propose a working model to explain the role of WRKY55 in age-triggered leaf senescence and the defense response (Fig. 11). Taken together, our work has clearly identified WRKY55 as a new WRKY TF for a complex regulatory network functioning in both leaf senescence and the defense response. In the future, it will be interesting to identify the upstream signaling pathways that control the expression and/or the activity of WRKY55 in addition to the interconnectivity of the downstream regulatory network.

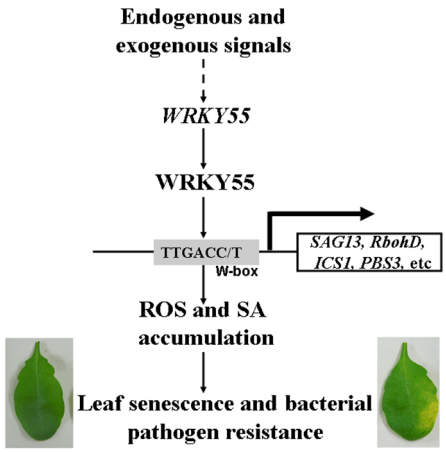

Fig. 11. A working model of WRKY55 in regulation of leaf senescence and pathogen resistance. Endogenous and exogenous signals can induce the expression of *WRKY55*. WRKY55 binds directly to the promoters of *SAG13*, *RbohD*, *ICS1* and *PBS3* genes via W-box elements and induces their transcription. As a result, ROS and SA accumulate, which triggers leaf senescence and resistance to the bacterial pathogen *Pst* DC3000. Arrows indicate positive regulations.

Development (2020) 147, dev189647. doi:10.1242/dev.189647

MATERIALS AND METHODS

Plant materials and growth conditions

Arabidopsis thaliana (ecotype Col-0) and *N. benthamiana* seeds were used in this study. Mutants seeds were obtained from NASC (Nottingham, UK). The *sid2-2* mutant was described previously (Dewdney et al., 2000). Seeds were surface sterilized and sown on half-strength MS medium supplemented with 0.8% Phytoblend (Caisson Labs). After being stratified at 4°C for 2 days, seed plates were placed in a growth chamber for germination. Seven-day-old seedlings were transferred into soil mix. The growth conditions were 22°C, with a photoperiod of 14 h light/10 h dark, a light intensity of ∼120 µE m^{-2} s^{-1} and a relative humidity of 60-70%. The T-DNA insertion mutants were screened and confirmed through PCR and RT-PCR. Flanking sequences of T-DNA mutants generated by LBb1.3 and RP primers were cloned into pJET1.2 vector (Fermentas, USA) and sequenced.

RT-PCR and qRT-PCR

Fourteen-day-old *Arabidopsis* seedlings were used for total RNA extraction using a Plant RNA kit (Omega Bio-tek, USA). The RNA was treated with DNaseI included in the DNA-free kit (Fermentas) before being used in RT. First-strand complementary DNA synthesis and high-fidelity PCR amplification using PrimeSTAR HS DNA polymerase (TaKaRa, Japan) were performed as previously described (Liang et al., 2013). The primers used are listed in Table S1. The PCR products were purified and cloned into destination vectors before being sequenced.

For expression analysis during leaf development, rosette leaves of soil-grown WT plants were harvested on different days post-stratification, namely 21 (young leaves), 28 (mature leaves), 35 (early senescent leaves) and 42 dps (late senescent leaves), for a total of three biological replicates. The tip, middle and base sections of 42-day-old rosette leaves were also separated and stored at −80°C before use. For qRT-PCR analysis, total RNA was extracted as described previously. Total RNA (2.5-5 µg) was reverse transcribed in a 20 µl reaction mixture using oligo$(dT)_{18}$ and RNase H^- MMLV (TaKaRa). The resultant complementary DNA was diluted and subjected to relative quantitative PCR using the SYBR Green I premix (CWbio) on a CFX96 thermocycler (Bio-Rad). As internal controls, the *UBQ10* and *UBC21* transcripts were used to normalize expression levels of target genes in each sample (Jiang and Deyholos, 2009). Three biological replicates were conducted. The primers used are listed in Table S1.

Transcriptional activity assay in yeasts

The coding region of *WRKY55* was cloned into the pGBKT7 (BD) vector (Clontech Laboratories), using the primers listed in Table S1. The assay in yeast was performed as described previously (Wang et al., 2015).

Dual luciferase reporter assay

The coding region of *WRKY55* was subcloned into the pYJHA plasmid, which was modified from pCsGFPBT. Reporter plasmid 5xW-box::LUC contains tandem repeats of the W-box element and the minimal TATA region of the 35S promoter of CaMV, which are located upstream of the *fLUC* gene in the pGreenII0800-LUC vector (Hellens et al., 2005). Individual promoters [including the 5′ untranslated region (UTR)] of genes of interest were cloned by PCR using PrimeSTAR HS DNA polymerase and genomic DNA of Col-0 as the template. After restriction, promoters were cloned to pGreenII0800-LUC before being confirmed by sequencing. The internal control was *Renilla* luciferase (rLUC) driven by the 35S promoter. The control plasmid was a binary vector pYJHA-GFP, in which expression of the *GFP* gene was controlled by the CaMV35S promoter. All plasmids were introduced into *Agrobacterium tumefaciens* strain GV3101 (pSoup) individually through a freeze-thaw method, and agrobacterial cultures transformed with the effector and reporter plasmid (9:1, v/v) were co-infiltrated into the lower epidermal side of 30-day-old *N. benthamiana* leaves. At 2 and 3 dpi, leaf disks with a diameter of 1 cm were harvested, ground in liquid nitrogen and extracted in 300 µl of lysis buffer, with the supernatant being used to assay LUC and REN activity with the dual luciferase assay kit according to the manufacturer's instructions (Promega) on a GloMax 20-20 luminometer (Promega). The ratio of fLUC to rLUC was calculated, and three biological replicates were assayed.

Subcellular localization

To examine the localization of WRKY55 *in planta*, the coding region was fused upstream of *GFP* in the pYJGFP vector. Transformed *Agrobacterium tumefaciens* GV3101 (pMP90) culture was resuspended in infiltration medium before infiltration into 30-day-old leaves of *N. benthamiana* (Liang et al., 2013). Two days later, leaf disks were observed for GFP signals under a confocal microscope (FV1000MPE; Olympus).

Constitutive and inducible overexpression

For the construction of plants with estradiol-responsive transgene expression (XVE), the open reading frames of *WRKY55* and *GUS* were subcloned into the binary vector pER8-3xHA, modified from pER8 (Zuo et al., 2000). For constitutive overexpression, the coding region of *WRKY55* and *GFP* was subcloned into the pYJHA vector. After verification by sequencing, the constructs were transformed into *Agrobacterium tumefaciens* strain GV3101 (pMP90), which was then used for the transformation of WT Col-0 plants by the floral dip method (Clough and Bent, 1998). Transgenic plants were selected with the use of 25 mg l^{-1} hygromycin B (Roche). Expression levels of genes were analyzed through qRT-PCR. Seeds of homozygous T3 generation plus control genotypes grown at the same time in identical conditions were used for phenotypic assay. The expression of *WRKY55* and *GUS* was induced using 5-10 µM BE (Sigma) for a designated duration.

Leaf senescence assays

For any phenotypic assay, seeds were harvested from plants of different genotypes (including WT and other controls) that were grown at the same time in long-day growth conditions. Leaves of plants with different genotypes grown in soil mix in the same conditions at the same time were used for the leaf senescence assay or sampled for physiological measurements. Electrolyte leakage was measured according to Sun et al. (2014). The distribution of H_2O_2 was detected by DAB staining according to the previously described protocol (Sun et al., 2014). Total chlorophyll was extracted in absolute ethanol in the dark at 4°C. Relative chlorophyll levels were determined by fluorescence using a spectrometer (Thermo Scientific). H_2O_2 was quantified as described previously (Rehmani et al., 2019).

RNA-seq analysis

Plants of *WRKY55*-IOE#13 and *GUS*-IOE were grown in normal conditions at 22°C for 14 days. After induction with BE (10 µM) for 2 days, samples were harvested, flash frozen in liquid nitrogen and stored at −80°C. Samples of three biological replicates were prepared. RNA-seq was performed by CapitalBio. In brief, RNA was extracted using a plant RNA kit (Tiangen) and, after purification, sequencing libraries were constructed using NEBNext Ultra RNA Library Prep Kit for Illumina (#E7530L; NEB) following the manufacturer's manual. After cluster generation, the libraries were sequenced on an Illumina HiSeq 2000 platform. Raw data were processed with Perl scripts to ensure the quality for follow-up analyses. A filtering criterion was applied to remove adapter-polluted reads, reads containing more than five adapter-polluted bases and low-quality reads. The clean data obtained were subjected to statistical analyses. The high-quality reads were then mapped to the *Arabidopsis thaliana* reference genome sequence (TAIR10) with the program TopHat (v.2.0.12). DESeq (v.1.16) was used to identify the DEGs via a model based on the negative binomial distribution. A *P*-value was assigned to each gene and adjusted to control the false-discovery rate. The GO (http://geneontology.org/) enrichment analysis of DEGs was performed by the hypergeometric test, in which the *P*-value is calculated and adjusted to a *q*-value. GO terms with $q<0.05$ were considered to be significantly enriched. The Integrative Genomics Viewer (http://software.broadinstitute.org/software/igv) was used to visualize the reads for selected genes.

Electrophoretic mobility shift assay

For expression in *E. coli*, the coding sequence of *WRKY55* was subcloned into the pGEX 4T-1 vector and transferred into the *E. coli* strain Rosetta (DE3) (Novagen). The expression of GST-WRKY55 or GST (from the empty vector) was induced by 0.1 mM isopropyl-β-D-1-thiogalactopyranoside

Development (2020) 147, dev189647. doi:10.1242/dev.189647

(IPTG) at 20°C for 12 h. The recombinant proteins were purified with GST-bind resin (Novagen) according to the manufacturer's instructions. Probes were generated by high-fidelity *Pfu* DNA polymerase (Bioer)-mediated PCR or annealing of short oligos, which were labeled with biotin at the 3′ end using the Biotin 3′End DNA Labeling Kit (Pierce). EMSA was performed with the Light Shift Chemiluminescent EMSA Kit (Pierce). Relevant primers are listed in Table S1. Unlabeled competitors were added in 5- to 200-fold molar excess. Images were captured on a ChemDoc system (Bio-Rad).

ChIP-qPCR

ChIP was performed as described previously (Saleh et al., 2008). Briefly, pER8HA-*GUS* and pER8HA-*WRKY55* transgenic seeds were sterilized and grown on solid half-strength MS medium for 10 days before being treated with 10 µM BE for 2 days. Harvested seedlings (3-4 g) were fixed in 1% formaldehyde for 15 min and neutralized with 0.125 M glycine for an additional 5 min. After washing twice with sterilized water, tissues were ground in liquid nitrogen. Chromatin DNA was then isolated and sonicated. Sonicated chromatin supernatant was diluted, and 20 µl of protein A-agarose bead (Upstate) was added for preclearing at 4°C for 1 h. Twenty microliters of anti-HA antibody (Cat# H6908, Lot# 077M4854V; Sigma) was added before incubation at 4°C for 14-16 h. The salmon sperm DNA/protein A-agarose beads were added and gently rotated at 4°C for 4 h. After washing with low-salt and high-salt wash buffers and Tris-EDTA buffer, the DNA was eluted and subjected to reverse cross-linking. Eluates were treated with proteinase K (Sigma) for 3 h at 37°C to remove proteins, with DNA being extracted by a phenol/chloroform approach and precipitated with the aid of glycogen (Fermentas). The purified DNA was resuspended in sterile water. The enrichment of DNA fragments was determined by qPCR using primers listed in Table S1. Gene-specific primers annealing to regions located ≥1 kb downstream of the translational start site were used as controls. The final results are presented as a percentage of the input DNA. A total of four biological replicates were prepared and analyzed.

SA measurement

The rosette leaves (~150 mg) of mutants and WT were harvested from 30-day-old soil-grown plants. For inducible overexpression lines, plants were sprayed with 10 µM BE for 5 days before being sampled. Three or four biological replicates were prepared for each genotype. Samples were flash-frozen in liquid nitrogen, with SA contents being quantified as described previously (Wu et al., 2007). In brief, 1 ml ethyl acetate containing 200 ng $^{2}H_{4}$-SA (used as an internal standard for SA) was added to each sample. Samples were then homogenized using a homogenizer. Next, the homogenized samples were centrifuged at 16,100 ***g*** for 10 min at 4°C and the supernatants transferred to 2 ml tubes. The precipitate was extracted with 0.5 ml ethyl acetate again, and the supernatants were combined and evaporated to dryness using a vacuum concentrator. The residue of each sample was resuspended in 0.5 ml of 70% methanol (v/v), centrifuged at 16,100 ***g*** for 15 min, and the supernatants were transferred into glass vials and used for detection on an ultra-performance liquid chromatography system with a Shim-pack XR-ODS (2.0 mm inner diameter ×75 mm long, 1.6 µm particle diameter) column coupled to a triple quadrupole mass spectrometer (LC-MS8040; Shimadzu, Japan) with an electrospray source (ESI).

Bacterial pathogen inoculation assay

Mature rosette leaves of 1-month-old plants of different genotypes were used for *Pst* DC3000 strain inoculations using a 1 ml needleless syringe as described by Katagiri et al. (2002). Infiltrated leaves were harvested at 0 (immediately after infiltration) and 3 dpi and homogenized in 10 mM $MgCl_2$. Tenfold serial dilutions of leaf extracts were performed, dropped on King's B medium supplemented with 25 mg/l rifampicin and incubated at 28°C for 2 days before the colony forming units (cfu) per square centimeter were determined. Three biological replicates were prepared.

Statistical analysis

All experiments were repeated at least three times (three biological replicates). All data were analyzed statistically using Excel 2003 or SPSS v.16.0.

Acknowledgements

We thank NASC for providing the mutant seeds, Shao-Kai Ning for technical help, Drs Nam-Hai Chua (Rockefeller University) for providing the pER8 vector and Shuhua Yang (China Agricultural University) for the *Pst* DC3000 strain, Jian-Qiang Wu and Jinfeng Qi (Kunming Institute of Botany, CAS) for technical help.

Competing interests

The authors declare no competing or financial interests.

Author contributions

Conceptualization: Y.-Q.J., B.Y.; Methodology: Y.-Q.J., B.Y.; Software: Y.-Q.J.; Validation: Y.W.; Formal analysis: Y.W., X.C., Y.-Q.J.; Investigation: Y.W., X.C., B.Y., S.X., X.W., P.Z., M.S.; Resources: B.Y., F.N., C.W., H.C., Y.-Q.J.; Data curation: Y.W., X.C., Y.-Q.J.; Writing - original draft: Y.-Q.J.; Writing - review & editing: B.Y., Y.-Q.J.; Supervision: Y.-Q.J., B.Y.; Project administration: B.Y., Y.-Q.J.; Funding acquisition: Y.-Q.J., B.Y.

Funding

This study was financially supported by the National Natural Science Foundation of China [31270293 and 31471153 to Y.-Q.J., and 31301648 to B.Y.], by the Fundamental Research Funds for the Central Universities [2452016080 to Y.-Q.J.] and by the Open Project of State Key Laboratory of Soil Erosion and Dryland Farming on the Loess Plateau, Institute of Water and Soil Conservation [A314021402-1505].

Data availability

RNA-seq raw data have been deposited in the Sequence Read Archive (SRA) database (https://www.ncbi.nlm.nih.gov/sra) under the accession number PRJNA606681. Sequence data from this article can be found on the TAIR website (https://www.arabidopsis.org) under the following AGI codes: *WRKY55* (At2g40740), *ICS1* (At1g74710), *RbohA* (At5g07390), *RbohB* (At1g09090), *RbohD* (At5g47910), *RbohF* (At1g64060), *RbohI* (At4g11230), *SAG13* (At2g29350), *SAG29* (At5g13170), *PBS3* (At5g13320), *PR1* (At2g14610), *PR5* (At1g75040), *ICS2* (At1g18870), *EDS5* (At4g39030), *UBQ10* (At4g05320), *WRKY75* (At5g13080), *UBC21* (At5g25760) and *ACTIN2* (At3g18780).

Supplementary information

Supplementary information available online at
https://dev.biologists.org/lookup/doi/10.1242/dev.189647.supplemental

Peer review history

The peer review history is available online at
https://dev.biologists.org/lookup/doi/10.1242/dev.189647.reviewer-comments.pdf

References

Aarts, N., Metz, M., Holub, E., Staskawicz, B. J., Daniels, M. J. and Parker, J. E. (1998). Different requirements for EDS1 and NDR1 by disease resistance genes define at least two R gene-mediated signaling pathways in Arabidopsis. *Proc. Natl. Acad. Sci. USA* **95**, 10306-10311. doi:10.1073/pnas.95.17.10306

Adachi, H., Nakano, T., Miyagawa, N., Ishihama, N., Yoshioka, M., Katou, Y., Yaeno, T., Shirasu, K. and Yoshioka, H. (2015). WRKY transcription factors phosphorylated by MAPK regulate a plant immune NADPH oxidase in Nicotiana benthamiana. *Plant Cell* **27**, 2645-2663. doi:10.1105/tpc.15.00213

Balazadeh, S., Riaño-Pachón, D. M. and Mueller-Roeber, B. (2008). Transcription factors regulating leaf senescence in Arabidopsis thaliana. *Plant Biol. (Stuttg.)* **10** Suppl. 1, 63-75. doi:10.1111/j.1438-8677.2008.00088.x

Baxter, A., Mittler, R. and Suzuki, N. (2014). ROS as key players in plant stress signalling. *J. Exp. Bot.* **65**, 1229-1240. doi:10.1093/jxb/ert375

Besseau, S., Li, J. and Palva, E. T. (2012). WRKY54 and WRKY70 co-operate as negative regulators of leaf senescence in Arabidopsis thaliana. *J. Exp. Bot.* **63**, 2667-2679. doi:10.1093/jxb/err450

Breeze, E., Harrison, E., McHattie, S., Hughes, L., Hickman, R., Hill, C., Kiddle, S., Kim, Y.-S., Penfold, C. A., Jenkins, D. et al. (2011). High-resolution temporal profiling of transcripts during Arabidopsis leaf senescence reveals a distinct chronology of processes and regulation. *Plant Cell* **23**, 873-894. doi:10.1105/tpc.111.083345

Buchanan-Wollaston, V., Page, T., Harrison, E., Breeze, E., Lim, P. O., Nam, H. G., Lin, J.-F., Wu, S.-H., Swidzinski, J., Ishizaki, K. et al. (2005). Comparative transcriptome analysis reveals significant differences in gene expression and signalling pathways between developmental and dark/starvation-induced senescence in Arabidopsis. *Plant J.* **42**, 567-585. doi:10.1111/j.1365-313X.2005.02399.x

Chen, H., Xue, L., Chintamanani, S., Germain, H., Lin, H., Cui, H., Cai, R., Zuo, J., Tang, X., Li, X. et al. (2009). ETHYLENE INSENSITIVE3 and ETHYLENE INSENSITIVE3-LIKE1 repress SALICYLIC ACID INDUCTION DEFICIENT2 expression to negatively regulate plant innate immunity in Arabidopsis. *Plant Cell* **21**, 2527-2540. doi:10.1105/tpc.108.065193

Chen, L., Xiang, S., Chen, Y., Li, D. and Yu, D. (2017). Arabidopsis WRKY45 interacts with the DELLA protein RGL1 to positively regulate age-triggered leaf senescence. *Mol Plant* **10**, 1174-1189. doi:10.1016/j.molp.2017.07.008

Ciolkowski, I., Wanke, D., Birkenbihl, R. P. and Somssich, I. E. (2008). Studies on DNA-binding selectivity of WRKY transcription factors lend structural clues into WRKY-domain function. *Plant Mol. Biol.* **68**, 81-92. doi:10.1007/s11103-008-9353-1

Clough, S. J. and Bent, A. F. (1998). Floral dip: a simplified method for Agrobacterium-mediated transformation of Arabidopsis thaliana. *Plant J.* **16**, 735-743. doi:10.1046/j.1365-313x.1998.00343.x

Daneva, A., Gao, Z., Van Durme, M. and Nowack, M. K. (2016). Functions and regulation of programmed cell death in plant development. *Annu. Rev. Cell Dev. Biol.* **32**, 441-468. doi:10.1146/annurev-cellbio-111315-124915

Demidchik, V., Straltsova, D., Medvedev, S. S., Pozhvanov, G. A., Sokolik, A. and Yurin, V. (2014). Stress-induced electrolyte leakage: the role of K+-permeable channels and involvement in programmed cell death and metabolic adjustment. *J. Exp. Bot.* **65**, 1259-1270. doi:10.1093/jxb/eru004

Dempsey, D., Vlotb, A., Wildermuthc, M. C. and Klessiga, D. (2011). Salicylic acid biosynthesis and metabolism. *in Arabidopsis Book* **9**, e0156. doi:10.1199/tab.0156

Dewdney, J., Reuber, T. L., Wildermuth, M. C., Devoto, A., Cui, J., Stutius, L. M., Drummond, E. P. and Ausubel, F. M. (2000). Three unique mutants of Arabidopsis identify eds loci required for limiting growth of a biotrophic fungal pathogen. *Plant J.* **24**, 205-218. doi:10.1046/j.1365-313x.2000.00870.x

Doll, J., Muth, M., Riester, L., Nebel, S., Bresson, J., Lee, H.-C. and Zentgraf, U. (2020). Arabidopsis thaliana WRKY25 transcription factor mediates oxidative stress tolerance and regulates senescence in a redox-dependent manner. *Front Plant Sci* **10**, 1734. doi:10.3389/fpls.2019.01734

Dong, J., Chen, C. and Chen, Z. (2003). Expression profiles of the Arabidopsis WRKY gene superfamily during plant defense response. *Plant Mol. Biol.* **51**, 21-37. doi:10.1023/A:1020780022549

Gan, S. and Amasino, R. M. (1997). Making sense of senescence (Molecular genetic regulation and manipulation of leaf senescence). *Plant Physiol.* **113**, 313-319. doi:10.1104/pp.113.2.313

Gepstein, S., Sabehi, G., Carp, M.-J., Hajouj, T., Nesher, M. F. O., Yariv, I., Dor, C. and Bassani, M. (2003). Large-scale identification of leaf senescence-associated genes. *Plant J.* **36**, 629-642. doi:10.1046/j.1365-313X.2003.01908.x

Guo, Y. and Gan, S. (2005). Leaf senescence: signals, execution, and regulation. *Curr. Top. Dev. Biol.* **71**, 83-112. doi:10.1016/S0070-2153(05)71003-6

Guo, Y., Cai, Z. and Gan, S. (2004). Transcriptome of Arabidopsis leaf senescence. *Plant Cell Environ.* **27**, 521-549. doi:10.1111/j.1365-3040.2003.01158.x

Guo, P., Li, Z., Huang, P., Li, B., Fang, S., Chu, J. and Guo, H. (2017). A tripartite amplification loop involving the transcription factor WRKY75, salicylic acid, and reactive oxygen species accelerates leaf senescence. *Plant Cell* **29**, 2854-2870. doi:10.1105/tpc.17.00438

Hellens, R. P., Allan, A. C., Friel, E. N., Bolitho, K., Grafton, K., Templeton, M. D., Karunairetnam, S., Gleave, A. P. and Laing, W. A. (2005). Transient expression vectors for functional genomics, quantification of promoter activity and RNA silencing in plants. *Plant Methods* **1**, 13. doi:10.1186/1746-4811-1-13

Hieno, A., Naznin, H. A., Inaba-Hasegawa, K., Yokogawa, T., Hayami, N., Nomoto, M., Tada, Y., Yokogawa, T., Higuchi-Takeuchi, M., Hanada, K. et al. (2019). Transcriptome analysis and identification of a transcriptional regulatory network in the response to H2O2. *Plant Physiol.* **180**, 1629-1646. doi:10.1104/pp.18.01426

James, M., Poret, M., Masclaux-Daubresse, C., Marmagne, A., Coquet, L., Jouenne, T., Chan, P., Trouverie, J. and Etienne, P. (2018). SAG12, a major cysteine protease involved in nitrogen allocation during senescence for seed production in Arabidopsis thaliana. *Plant Cell Physiol.* **59**, 2052-2063. doi:10.1093/pcp/pcy125

Jiang, Y. Q. and Deyholos, M. K. (2009). Functional characterization of Arabidopsis NaCl-inducible WRKY25 and WRKY33 transcription factors in abiotic stresses. *Plant Mol. Biol.* **69**, 91-105. doi:10.1007/s11103-008-9408-3

Jiang, Y., Liang, G., Yang, S. and Yu, D. (2014). Arabidopsis WRKY57 functions as a node of convergence for jasmonic acid- and auxin-mediated signaling in jasmonic acid-induced leaf senescence. *Plant Cell* **26**, 230-245. doi:10.1105/tpc.113.117838

Katagiri, F., Thilmony, R. and He, S. Y. (2002). The Arabidopsis thaliana-pseudomonas syringae interaction. *Arabidopsis Book* **1**, e0039. doi:10.1199/tab.0039

Kim, K.-C., Fan, B. F. and Chen, Z. X. (2006). Pathogen-induced Arabidopsis WRKY7 is a transcriptional repressor and enhances plant susceptibility to Pseudomonas syringae. *Plant Physiol.* **142**, 1180-1192. doi:10.1104/pp.106.082487

Kim, H. J., Nam, H. G. and Lim, P. O. (2016). Regulatory network of NAC transcription factors in leaf senescence. *Curr. Opin. Plant Biol.* **33**, 48-56. doi:10.1016/j.pbi.2016.06.002

Kim, H. J., Park, J.-H., Kim, J., Kim, J. J., Hong, S., Kim, J., Kim, J. H., Woo, H. R., Hyeon, C., Lim, P. O. et al. (2018). Time-evolving genetic networks reveal a NAC troika that negatively regulates leaf senescence in Arabidopsis. *Proc. Natl. Acad. Sci. USA* **115**, E4930-E4939. doi:10.1073/pnas.1721523115

Koo, J. C., Lee, I. C., Dai, C., Lee, Y., Cho, H. K., Kim, Y., Phee, B.-K., Kim, H., Lee, I. H., Choi, S. H. et al. (2017). The protein trio RPK1-CaM4-RbohF mediates transient superoxide production to trigger age-dependent cell death in Arabidopsis. *Cell Rep.* **21**, 3373-3380. doi:10.1016/j.celrep.2017.11.077

Kwak, J. M., Mori, I. C., Pei, Z. M., Leonhardt, N., Torres, M. A., Dangl, J. L., Bloom, R. E., Bodde, S., Jones, J. D. and Schroeder, J. I. (2003). NADPH oxidase AtrbohD and AtrbohF genes function in ROS-dependent ABA signaling in Arabidopsis. *EMBO J.* **22**, 2623-2633. doi:10.1093/emboj/cdg277

Leon, J., Lawton, M. A. and Raskin, I. (1995). Hydrogen peroxide stimulates salicylic acid biosynthesis in tobacco. *Plant Physiol.* **108**, 1673-1678. doi:10.1104/pp.108.4.1673

Li, Z., Peng, J., Wen, X. and Guo, H. (2012). Gene network analysis and functional studies of senescence-associated genes reveal novel regulators of Arabidopsis leaf senescence. *J. Integr. Plant Biol.* **54**, 526-539. doi:10.1111/j.1744-7909.2012.01136.x

Liang, W., Yang, B., Yu, B.-J., Zhou, Z., Li, C., Sun, Y., Zhang, Y., Jia, M., Wu, F., Zhang, H. et al. (2013). Identification and analysis of MKK and MPK gene families in Canola (Brassica napus L.). *BMC Genomics* **14**, 392. doi:10.1186/1471-2164-14-392

Lim, P. O., Kim, H. J. and Nam, H. G. (2007). Leaf senescence. *Annu. Rev. Plant Biol.* **58**, 115-136. doi:10.1146/annurev.arplant.57.032905.105316

Miao, Y. and Zentgraf, U. (2007). The antagonist function of Arabidopsis WRKY53 and ESR/ESP in leaf senescence is modulated by the jasmonic and salicylic acid equilibrium. *Plant Cell* **19**, 819-830. doi:10.1105/tpc.106.042705

Miao, Y., Laun, T., Zimmermann, P. and Zentgraf, U. (2004). Targets of the WRKY53 transcription factor and its role during leaf senescence in Arabidopsis. *Plant Mol. Biol.* **55**, 853-867. doi:10.1007/s11103-005-2142-1

Morris, K., MacKerness, S. A.-H., Page, T., John, C. F., Murphy, A. M., Carr, J. P. and Buchanan-Wollaston, V. (2000). Salicylic acid has a role in regulating gene expression during leaf senescence. *Plant J.* **23**, 677-685. doi:10.1046/j.1365-313x.2000.00836.x

Nawrath, C., Heck, S., Parinthawong, N. and Métraux, J.-P. (2002). EDS5, an essential component of salicylic acid-dependent signaling for disease resistance in Arabidopsis, is a member of the MATE transporter family. *Plant Cell* **14**, 275-286. doi:10.1105/tpc.010376

Nühse, T. S., Bottrill, A. R., Jones, A. M. E. and Peck, S. C. (2007). Quantitative phosphoproteomic analysis of plasma membrane proteins reveals regulatory mechanisms of plant innate immune responses. *Plant J.* **51**, 931-940. doi:10.1111/j.1365-313X.2007.03192.x

O'Brien, J. A., Daudi, A., Butt, V. S. and Bolwell, G. P. (2012). Reactive oxygen species and their role in plant defence and cell wall metabolism. *Planta* **236**, 765-779. doi:10.1007/s00425-012-1696-9

Rao, M. V., Paliyath, G., Ormrod, D. P., Murr, D. P. and Watkins, C. B. (1997). Influence of salicylic acid on H2O2 production, oxidative stress, and H2O2-metabolizing enzymes. Salicylic acid-mediated oxidative damage requires H2O2. *Plant Physiol.* **115**, 137-149.

Rehmani, M. S., Chen, Q., Yan, J., Cui, X., Gao, S., Niu, F., Yang, L., Yang, B. and Jiang, Y.-Q. (2019). A novel stress-responsive BnaNAL1 transcriptional activator in oilseed rape positively modulates reactive oxygen species production and cell death. *Environ. Exp. Bot.* **163**, 1-14. doi:10.1016/j.envexpbot.2019.04.004

Rekhter, D., Lüdke, D., Ding, Y., Feussner, K., Zienkiewicz, K., Lipka, V., Wiermer, M., Zhang, Y. and Feussner, I. (2019). Isochorismate-derived biosynthesis of the plant stress hormone salicylic acid. *Science* **365**, 498-502. doi:10.1126/science.aaw1720

Ren, G., An, K., Liao, Y., Zhou, X., Cao, Y., Zhao, H., Ge, X. and Kuai, B. (2007). Identification of a novel chloroplast protein AtNYE1 regulating chlorophyll degradation during leaf senescence in Arabidopsis. *Plant Physiol.* **144**, 1429-1441. doi:10.1104/pp.107.100172

Rivas-San Vicente, M. and Plasencia, J. (2011). Salicylic acid beyond defence: its role in plant growth and development. *J. Exp. Bot.* **62**, 3321-3338. doi:10.1093/jxb/err031

Robatzek, S. and Somssich, I. E. (2001). A new member of the Arabidopsis WRKY transcription factor family, AtWRKY6, is associated with both senescence- and defence-related processes. *Plant J.* **28**, 123-133. doi:10.1046/j.1365-313X.2001.01131.x

Robatzek, S. and Somssich, I. E. (2002). Targets of AtWRKY6 regulation during plant senescence and pathogen defense. *Genes Dev.* **16**, 1139-1149. doi:10.1101/gad.222702

Rushton, P. J., Somssich, I. E., Ringler, P. and Shen, Q. J. (2010). WRKY transcription factors. *Trends Plant Sci.* **15**, 247-258. doi:10.1016/j.tplants.2010.02.006

Saleh, A., Alvarez-Venegas, R. and Avramova, Z. (2008). An efficient chromatin immunoprecipitation (ChIP) protocol for studying histone modifications in Arabidopsis plants. *Nat. Protoc.* **3**, 1018-1025. doi:10.1038/nprot.2008.66

Sarris, P. F., Duxbury, Z., Huh, S. U., Ma, Y., Segonzac, C., Sklenar, J., Derbyshire, P., Cevik, V., Rallapalli, G., Saucet, S. B. et al. (2015). A plant immune receptor detects pathogen effectors that target WRKY transcription factors. *Cell* **161**, 1089-1100. doi:10.1016/j.cell.2015.04.024

Seo, P. J., Park, J.-M., Kang, S. K., Kim, S.-G. and Park, C.-M. (2011). An Arabidopsis senescence-associated protein SAG29 regulates cell viability under high salinity. *Planta* **233**, 189-200. doi:10.1007/s00425-010-1293-8

Sun, Y., Wang, C., Yang, B., Wu, F., Hao, X., Liang, W., Niu, F., Yan, J., Zhang, H., Wang, B. et al. (2014). Identification and functional analysis of mitogen-activated protein kinase kinase kinase (MAPKKK) genes in canola (Brassica napus L.). *J. Exp. Bot.* **65**, 2171-2188. doi:10.1093/jxb/eru092

Suzuki, N., Miller, G., Morales, J., Shulaev, V., Torres, M. A. and Mittler, R. (2011). Respiratory burst oxidases: the engines of ROS signaling. *Curr. Opin. Plant Biol.* **14**, 691-699. doi:10.1016/j.pbi.2011.07.014

Suzuki, N., Koussevitzky, S., Mittler, R. and Miller, G. (2012). ROS and redox signalling in the response of plants to abiotic stress. *Plant Cell Environ.* **35**, 259-270. doi:10.1111/j.1365-3040.2011.02336.x

Torrens-Spence, M. P., Bobokalonova, A., Carballo, V., Glinkerman, C. M., Pluskal, T., Shen, A. and Weng, J.-K. (2019). PBS3 and EPS1 complete salicylic acid biosynthesis from isochorismate in Arabidopsis. *Mol. Plant* **12**, 1577-1586. doi:10.1016/j.molp.2019.11.005

Torres, M. A. and Dangl, J. L. (2005). Functions of the respiratory burst oxidase in biotic interactions, abiotic stress and development. *Curr. Opin. Plant Biol.* **8**, 397-403. doi:10.1016/j.pbi.2005.05.014

Torres, M. A., Dangl, J. L. and Jones, J. D. G. (2002). Arabidopsis gp91phox homologues AtrbohD and AtrbohF are required for accumulation of reactive oxygen intermediates in the plant defense response. *Proc. Natl. Acad. Sci. USA* **99**, 517-522. doi:10.1073/pnas.012452499

Ülker, B. and Somssich, I. E. (2004). WRKY transcription factors: from DNA binding towards biological function. *Curr. Opin. Plant Biol.* **7**, 491-498. doi:10.1016/j.pbi.2004.07.012

van der Graaff, E., Schwacke, R., Schneider, A., Desimone, M., Flügge, U.-I. and Kunze, R. (2006). Transcription analysis of arabidopsis membrane transporters and hormone pathways during developmental and induced leaf senescence. *Plant Physiol.* **141**, 776-792. doi:10.1104/pp.106.079293

Vlot, A. C., Dempsey, D. M. A. and Klessig, D. F. (2009). Salicylic acid, a multifaceted hormone to combat disease. *Annu. Rev. Phytopathol.* **47**, 177-206. doi:10.1146/annurev.phyto.050908.135202

Wang, B., Guo, X., Wang, C., Ma, J., Niu, F., Zhang, H., Yang, B., Liang, W., Han, F. and Jiang, Y.-Q. (2015). Identification and characterization of plant-specific NAC gene family in canola (Brassica napus L.) reveal novel members involved in cell death. *Plant Mol. Biol.* **87**, 395-411. doi:10.1007/s11103-015-0286-1

Weaver, L. M., Gan, S., Quirino, B. and Amasino, R. M. (1998). A comparison of the expression patterns of several senescence-associated genes in response to stress and hormone treatment. *Plant Mol. Biol.* **37**, 455-469. doi:10.1023/A:1005934428906

Wildermuth, M. C., Dewdney, J., Wu, G. and Ausubel, F. M. (2001). Isochorismate synthase is required to synthesize salicylic acid for plant defence. *Nature* **414**, 562-565. doi:10.1038/35107108

Winter, D., Vinegar, B., Nahal, H., Ammar, R., Wilson, G. V. and Provart, N. J. (2007). An "Electronic Fluorescent Pictograph" browser for exploring and analyzing large-scale biological data sets. *PLoS ONE* **2**, e718. doi:10.1371/journal.pone.0000718

Woo, H. R., Kim, H. J., Nam, H. G. and Lim, P. O. (2013). Plant leaf senescence and death - regulation by multiple layers of control and implications for aging in general. *J. Cell Sci.* **126**, 4823-4833. doi:10.1242/jcs.109116

Woo, H. R., Koo, H. J., Kim, J., Jeong, H., Yang, J. O., Lee, I. H., Jun, J. H., Choi, S. H., Park, S. J., Kang, B. et al. (2016). Programming of plant leaf senescence with temporal and inter-organellar coordination of transcriptome in Arabidopsis. *Plant Physiol.* **171**, 452-467. doi:10.1104/pp.15.01929

Woo, H. R., Kim, H. J., Lim, P. O. and Nam, H. G. (2019). Leaf senescence: systems and dynamics aspects. *Annu. Rev. Plant Biol.* **70**, 347-376. doi:10.1146/annurev-arplant-050718-095859

Wu, J., Hettenhausen, C., Meldau, S. and Baldwin, I. T. (2007). Herbivory rapidly activates MAPK signaling in attacked and unattacked leaf regions but not between leaves of Nicotiana attenuata. *Plant Cell* **19**, 1096-1122. doi:10.1105/tpc.106.049353

Xu, X., Chen, C., Fan, B. and Chen, Z. (2006). Physical and functional interactions between pathogen-induced Arabidopsis WRKY18, WRKY40, and WRKY60 transcription factors. *Plant Cell* **18**, 1310-1326. doi:10.1105/tpc.105.037523

Zhang, Y. and Li, X. (2019). Salicylic acid: biosynthesis, perception, and contributions to plant immunity. *Curr. Opin. Plant Biol.* **50**, 29-36. doi:10.1016/j.pbi.2019.02.004

Zhang, H. and Zhou, C. (2013). Signal transduction in leaf senescence. *Plant Mol. Biol.* **82**, 539-545. doi:10.1007/s11103-012-9980-4

Zhang, K., Xia, X., Zhang, Y. and Gan, S.-S. (2012). An ABA-regulated and Golgi-localized protein phosphatase controls water loss during leaf senescence in Arabidopsis. *Plant J.* **69**, 667-678. doi:10.1111/j.1365-313X.2011.04821.x

Zhang, S., Li, C., Wang, R., Chen, Y., Shu, S., Huang, R., Zhang, D., Li, J., Xiao, S., Yao, N. et al. (2017). The Arabidopsis mitochondrial protease FtSH4 is involved in leaf senescence via regulation of WRKY-dependent salicylic acid accumulation and signaling. *Plant Physiol.* **173**, 2294-2307. doi:10.1104/pp.16.00008

Zhou, N., Tootle, T. L., Tsui, F., Klessig, D. F. and Glazebrook, J. (1998). PAD4 functions upstream from salicylic acid to control defense responses in Arabidopsis. *Plant Cell* **10**, 1021-1030. doi:10.1105/tpc.10.6.1021

Zuo, J., Niu, Q.-W. and Chua, N.-H. (2000). An estrogen receptor-based transactivator XVE mediates highly inducible gene expression in transgenic plants. *Plant J.* **24**, 265-273. doi:10.1046/j.1365-313x.2000.00868.x